Synthesis of Molecular Adducts for Studies of Electron Transfer Reactions

by

César Vitório Franco

Submitted in Partial Fulfillment
of the
Requirements for the Degree

DOCTOR OF PHILOSOPHY

Supervised by Dr. George McLendon
Department of Chemistry
College of Arts and Science

University of Rochester
Rochester, New York

1985

Acknowledgement

Curriculum Vitae

The author was born in Blumenau, Santa Catarina State, Brazil, April 11, 1954. He received his B.S. Degree from FURB (Fundação Universidade Regional de Blumenau) in 1977 and his Master of Science from UNICAMP (Universidade Estadual de Campinas) in 1980.

The author was a "Professor Assistente" at the Universidade Federal de Santa Catarina from 1980 through 1981. In late 1981, he entered the graduate program in chemistry at the University of Rochester, where he did his graduate work under the supervision of Dr. George McLendon. In 1984 he received a grant from the American Chemical Society to participate in the 188 th national meeting of the American Chemical Society in Philadelphia where he presented a talk about his graduate research. He is a coauthor of the following publications:

C. Franco and N. Duran, "Interaction of Thiocarbamates with indole-3-acetic acid peroxidase system", _Quim Nova_, _3_, 44 (1980).

C. Franco and N. Duran, "Metabolites of Carbofuran: Effect on Indole-3-acetic acid Metabolism", _Pesticide Biochemistry and Physiology_, _16_, 136, (1982).

ii

F. Nome, A. F. Rubira, C. Franco and L.C. Ionescu. "Limitations of the pseudo phase model of micelar catalysis. The Dehydrochorination of 1,1,1-trichloro-2,2 bis (p-chloro phenil) ethane and some of its derivatives", J. Phys. Chem., 86, 1981, (1982).

N. Duran, C. Franco and S. M. DeToledo. "Effect of Thiocarbamates on Indole-3-Acetic Acid Degradation", Brazilien J. Med. Biol. Res., 16, 17, (1983).

M. C. Rezende, A. F. Rubira, C. Franco, and F. Nome. "Effect of Normal and Functional Micelles in Elimination Reactions of Polhyalogenated Pesticides", J. Chem. Soc. Perkin Trans. II, 1075 (1983).

C. Franco and G. McLendon. "Bimetallic Perphyrin: Synthesis and Rapid Intramolecular Electron Transfer of meso-Tritolyl [N-(pentaammineruthenio)pyridyl]porphyrin". Inorg. Chem., 23, 2370-2372, (1984).

Dedication

To my Loving wife

Eliete

and our children

Daniela and Rafael

Abstract

A new cl.... of bifunctional red.x active porphyrins based on meso tritolyl monopyridyl porphyrin has been synthesized and characterized. In these compounds the meso pyridyl group ~~vides a lig..d for a second redox active metal site yielding the [meso (tritolyl)(monop;ridyl Ru(III)(NH_3)$_4$L') porphyrin], of the general structure:
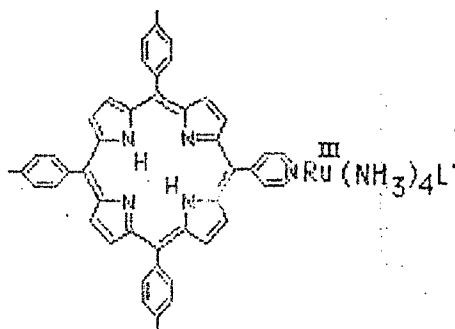
where L' = NH_3, pyridine, 3-Cl-pyric ne.

Porphyrin triplet excited state kinetics show that the triplet excited state of the porphyrin is quenched by the ruthenium moiety. This quenching process is attributed to the intramolecular electron transfer from porphyrin to Ruthenium with rates which depend on driving force as follows: For L = NH_3 $\Delta E = 0.37$, $k = 4 \times 10^4 s^{-1}$, L' = pyridine $\Delta E = 0.55 Y$, $k = 1.2 \times 10^5 s^{-1}$ and L = 3-Cl-pyridine $\Delta E = 0.65 Y$, $k = 5 \times 10^5 s^{-1}$.

Studies involving collisional _intermolecular_ quenching of the unsubstituted porphyrin

by $Ru(III)(NH_3)_5Py$ are compared with the collisionless, intramolecular systems. The results show that the intermolecular rate exceeds the rate of the intramolecular process by a factor ≥ 100, with the inequality determined by the solubility of $Ru(III)(NH_3)_5Py$. The intramolecular rates are found to be extremely low when compared with redox processes for analogous porphyrin quinone systems. Possible reasons for these differences are discussed.

Table of Contents

List of Tables

List of Figures

CHAPTER III

CHAPTER 1

Theory of Electron Transfer Reactions

INTRODUCTION

Studies in Electron transfer (ET) reactions, have long been a subject of intensive theoretical and experimental studies. The succesful interplay between theory and experiment in the area of electron transfer reaction makes possible advances in the design of solar energy devices, superconduction and semiconduction, as well as in the understanding of a wide variety of chemical, biological and microelectronic systems. The present success in comprehending and manipulating electron transfer events are due to the pioneering work of Marcus [1-4], Levich and Dognonadze [5], and Hush[6-7], and, more recently, work based on quantum mechanics and time-dependent perturbation theory [8-18].

Studies of natural photosynthetic centers over the last decades have brought considerable and intriguing data to inorganic biochemistry [24-29]. Indeed, inorganic redox reactions are of primary importance in biological systems. These transition metal complexes provide a wide range of oxidation states available over a comparatively narrow energy range which make them versatile redox reagents.

The present work will foccus on the design and synthesis of systems which mimic biological ET. An understanding of such systems could lead to the systematic development of new families of catalytic reagents, which could be used, for example, in photoconvertion of solar energy.

Beyond the important goal of development of catalysts for photoproduction of

hydrogen, other redox pathways play important roles in the oxidation of organic compounds, the interconversion of nitrate and nitrite, the oxidation of water to oxygen, the oxidation of Cl^- to Cl_2, the interconvertion of nitrite and ammonia [30], the reduction of N^{-3} to ammonia [31], the photoreduction of carbon dioxide [32], and the chain reactions initiated by a photoinduced electron transfer [33].

The emphasis in the present introduction is on photoinduced electron transfer where both the theoretical and practical aspects of photoinduced ET will be reviewed. Since the main changes in the redox properties of excited state molecules are independent of their type, whether they are organic or inorganic, an integrated treatment will be adopted that covers both types of species. The same treatment will be followed in the experimental part of this work. Here, the basic aim is to understand the process of ET in biological systems and provide new insight into the design of catalysts for photoconversion of solar energy.

The first section is devoted to the theory of electron transfer reactions with special emphasis on the classical theory which served as the guiding principle for work on electron transfer for more than two decades. Excellent reviews and monographs draw attention to the importance of this theory [2, 24, 34-37]. It is important to emphasize in this section the basis for photoelectron-transfer reactions and redox properties of excited states.

Section two describes the ET in biological systems with emphasis on the photosynthetic apparatus. A clear understanding of photosynthesis may lead to a new solution of the problems of energy storage.

A. THEORY OF ELECTRON TRANSFER REACTION

It is known that oxidation-reduction reactions of transition metal complexes can occur through two different mechanisms: (i) inner-sphere and (ii) outer-sphere. Such a distinction was introduced by Taube[38], and extended later to cover particular cases of organometallic and organic reactions[33,39-41]. An electron-transfer mechanism is said to be inner-sphere if the reductant and oxidant share one or more ligands of their first coordination spheres in the activated complex. The inner-sphere mechanism can occur with or without ligand exchange. However, the mechanism with ligand exchange is better known since it is easier to prove[42]. If an electron transfer reaction requires ligand exchange, it cannot be faster than ligand substitution reactions and is unlikely to occur within the lifetime of the photoexcited molecules[43]. To date, no example of photoinduced electron transfer by an inner sphere mechanism has been reported in the inorganic field. In the fields of organic and organometallic photochemistry the situation would be different if many photoinduced free-radical chain reactions were included in the general class of inner-sphere electron transfer. In the outer-sphere mechanism the electron transfer occurs with the first coordination sphere of the redox pair remaining intact, although the coordination sphere may change in a separate reaction subsequent to the redox reaction.

1. The Classical Theory of Electron Transfer Reaction

It is assumed in the classically based Marcus theory that all ET reactions occur on an adiabatic surface potential, which is formed by an avoided crossing of the reactants and products (Figure 1). Splitting of the two zero order surfaces by an interaction energy $2H_{ab}$ depends on the electronic states, the degree of shielding of the electronic orbitals, and the distance and orientation between the reactants. Figure 1 shows the profile of the potential-energy surface of reactants, $U_R(q)$, and products, $U_P(q)$, for two different degrees of adiabaticity. In this figure, the potential-energy surfaces are plotted versus the nuclear configuration which is represented by the value of q. Here the nuclear configuration includes the solvent and both reactants, and the potential-energy surface represents the center of mass of a multinuclear system, where a representative point moves with the same characteristics as a single particle. The path of the system is shown in Figure 2 by thick lines and arrows. Here the representative point can pass from q_R to q_P. The classical path of the transition is through q^*, which gives an indication of the horizontal displacement required to achieve the electron transfer. This is a consequence of the Franck-Condon principle which separates nuclear motion from electronic motion. The energy required to move all of he nuclei from equilibrium to the transition state q^* is the quantity E_{act}. Marcus[1-4] separates the total reorganization energy E_r into two parts, λ_{in} and λ_{out} which represent the inner- sphere effects and outer-sphere effects, respectively. These effects are also called

Figure 1. Potential-energy surfaces of reactants $U_R(q)$ and products $U_P(q)$ for an electron transfer process showing two different degrees of adiabaticity.
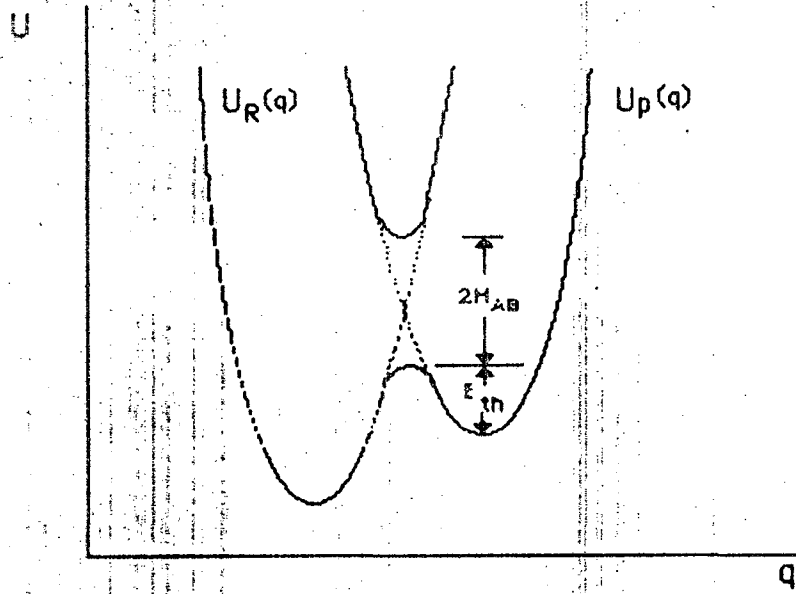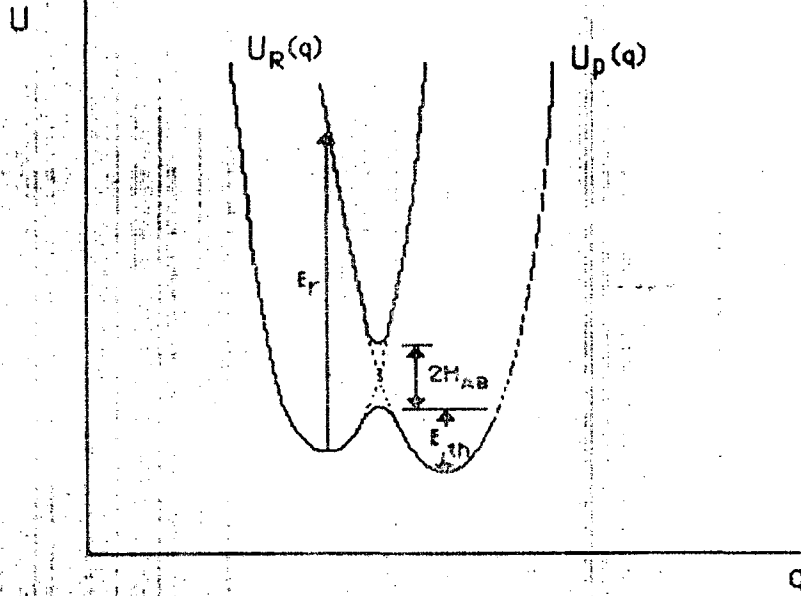
Figure 2. Potential-energy surfaces of reactant and products showing the electron transfer pathway and corresponding changes in the nuclear coordinates.
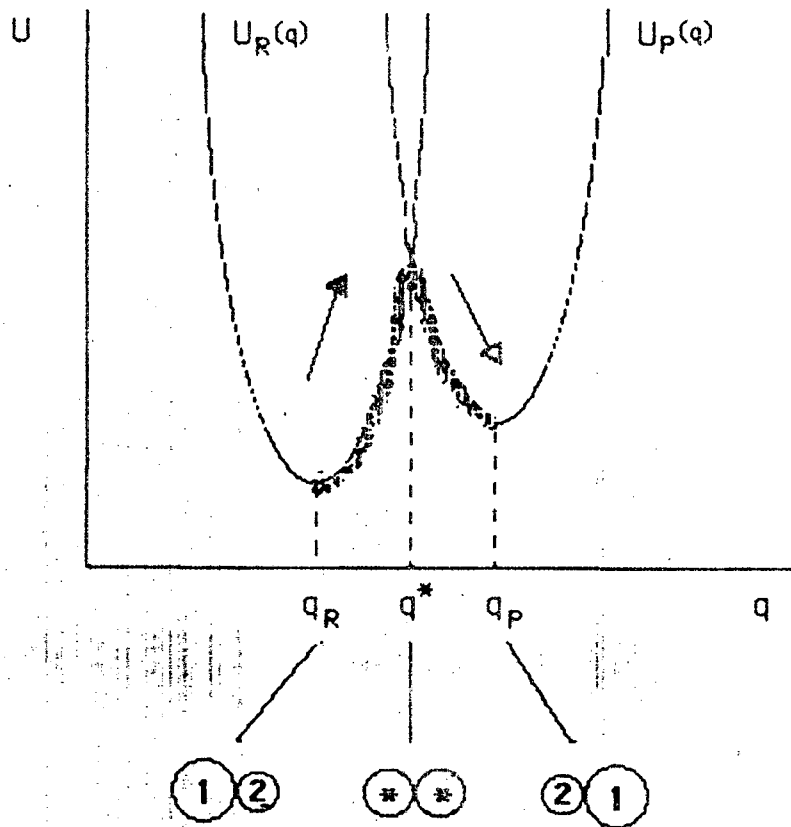
the inner and outer sphere reorganization energies and are important characteristics of electron transfer reactions since they determine, to a great extent, the height of the activation barrier at the intersection point q^*. These two types of rearranged vibrational modes are low-frequency ($<100 cm^{-1}$) polarization modes for λ_{out} and high-frequency ($\approx 500-3000$ cm^{-1}) bond vibrations for λ_{in} [44]. The inner-shell reorganization energy is classically calculated, using equation (1), by considering the inner shell vibrational modes as displaced harmonic oscillators:

$$\lambda_{in} = \frac{1}{2} \sum_i F_i Q_i^2 \qquad (1)$$

where F_i is the Hooke's law force constant for the ith inner-sphere vibration and Q_i is the displacement from the equilibrium position of the vibrational coordinates caused by the electron transfer. Assuming the solvent to be a continuous polar medium, the outer-sphere reorganization energy can be then estimated from the polarizability of the solvent and is given by equation (2),

$$\lambda_{out} = (\Delta e)^2/4\pi\epsilon_0 \left(\frac{1}{2a_1} + \frac{1}{2a_2} - \frac{1}{r_{12}} \right)\left(\frac{1}{D_{op}} - \frac{1}{D_s} \right) \qquad (2)$$

where Δe is the charge transfered from donor to acceptor, a_1 and a_2 are the radii of the two reactants when in contact, $r_{12} = r_1 + r_2$, ϵ_0 is the permittivity of the medium, and D_{op} and D_s are the square of the refractive indices of the medium and static dielectric constant, respectively.

In solution the rate constant, k may be written as

$$k = \frac{KT}{h} \kappa \exp(-\Delta G^*/KT) = \frac{KT}{h} \kappa \exp(-\Delta S^*/K)\exp(-\Delta H^*/KT) \qquad (3)$$

where κ, represents the electron-transfer 'matrix element' which determines the probability of electron-transfer between redox couples.

It has the value 1 for adiabatic reactions and ≤ 1 for non-adiabatic reactions. The other symbols in the equation have their usual meanings: ΔG^*, ΔS^*, ΔH^* are the free energy, entropy, enthalpy and K is the Boltzmann constant. Assuming a self exchange reaction, ΔG^* can be calculated by the Marcus equation:

$$\Delta G^* = \frac{(\Delta G + E_r)^2}{4 E_r} \tag{4}$$

where E_r is the total reorganization energy and ΔG is the overall free energy change. The work term which is the energy required to bring the reactants together is neglected. For a constant value of the reorganization energy, as it is shown from equation (4), as the value of ΔG increases, rate increases up to a maximum and then decreases. This is a central prediction of Marcus theory; thus the region of high exothemicity is called the "Marcus inverted region". In Figure 3 the representation of the classical dependence of rate on ΔG is shown. The dashed horizontal curve is for a diffusion-controlled limit which is responsible for the disappearence of the energetic information in fluid solution.

The above equation for the cross-reaction is also written as:[3,34,45-46]

$$\Delta G^*_{12} = \frac{(\Delta G^*_1 + \Delta G^*_2)}{2} + \frac{\Delta G}{2} + \frac{(\Delta G)^2}{8(\Delta G^*_1 + \Delta G^*)} \tag{5}$$

where ΔG^*_1 and ΔG^*_2 refer to the free energy of activation for the corresponding self-exchange reactions 6 and 7 and ΔG is the free energy change.

Figure 3. Plot of the logarithm of the activation-controlled (continuous line)
and diffusion-limited (dashed line) rate constants as a function of
increasing exothermicity, according to the classical model.

$$A_1 + A_1^+ \xrightleftharpoons{K_1} A_1^+ + A_1 \tag{6}$$

$$A_2 + A_2^- \xrightleftharpoons{K_2} A_2 + A_2^- \tag{7}$$
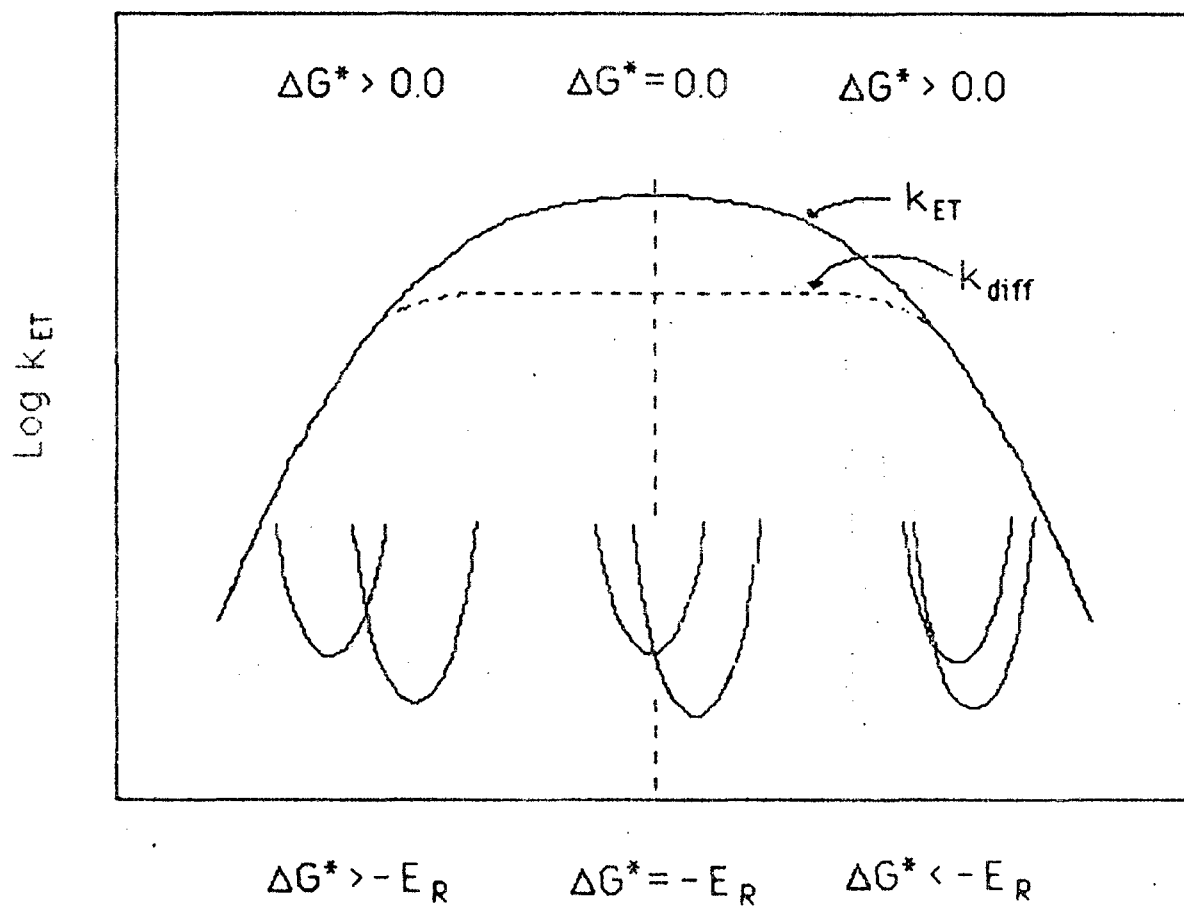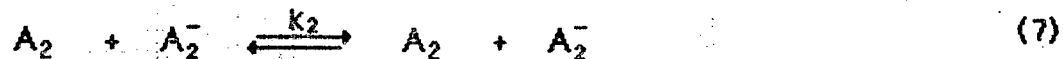
Equation (5) can be written as

$$\Delta G_{12}^x = E_r / 4 \, (1 + \Delta G / E_r) \tag{8}$$

where

$$E_r = 2 \, (\Delta G_1^x + \Delta G_2^x) \tag{9}$$

and can be related to the rates of two different electron-exchange reaction yielding the following expression:

$$k_{12} = (k_1 k_2 K_{12} f)^{1/2} \tag{10}$$

where

$$f = (\log K_{12})^2 / 4 \log (k_1 k_2 / Z^2) \tag{11}$$

with K_{12} being the equilibrium constant for the cross reaction.

The classical Marcus-Hush theory succesfully explains electron transfer processes ranging from simple organic compounds and coordination compounds to proteins[47], and electrode surfaces[48]. In a modified form, the theory can predict the rates of both ground state and electronic excited state reactions[43]. However, it does not deal directly with reactants which are separated in space. Such reactions are common in biological redox centers and in solid state chemistry[25,29,49-52].

2. The Semiclassical Approximation

In the attempt to interpret the temperature dependence of the rate of the cytochrome c oxidation in C. vinosum [25], Hopfield developed a semiclassical theory of electron transfer reactions [53]. Hopfield used an analogy to the Förster-Dexter theory of energy transfer, to develop this adiabatic theory.

In Hopfield's derivation, the rate of electron transfer W (sec^{-1}) is given by

$$W = \frac{2\pi}{\hbar} |H_{ab}|^2 (1/2\pi\sigma^2)^{1/2} \exp(-(E_a - E_b - \Delta)^2 / 2\sigma^2) \qquad (12)$$

where

$$\sigma^2 = (K_a X_a^2 / 2) k T_a \coth T_a / 2T + (k_b X_b^2 / 2) k T_b \coth T_b / 2T$$

$$\Delta = 1/2 K_a X_a^2 + 1/2 k_b X_b^2$$

k = Boltzman's constant

T = Temperature in $^\circ K$

K_a and k_b are Hook's law force constant for vibrations of species a and b

and X_a and X_b represent displacement of nuclear coordinates from their equilibrium positions.

Here Δ reflects the barrier width, σ^2 the shape of the potential surface, and T_a, T_b is a tunneling matrix element which depends on orbital overlap. $E_a - E_b$ is the potential for the reaction.

This theory predicts that the electron transfer reaction rate will decrease exponentially with increasing distance, and at a fixed distance, the rate of electron transfer depends strongly on redox potential.

The results from the classical experiments by Chance and coworkers were shown by Hopfield[53] to be consistent with tunneling. However, the theory presents some aspects that are subject to criticism. For example, it has been suggested that electron transfer processes are far from being analogous to energy transfer[54,55]. Indeed, The Förster-Dexter theory[56,57] assumes that each donor and acceptor pair, couples to a different set of oscillators, whereas in electron transfer the movement of charge over a considerable distance would likely cause more disturbance to the medium. Consequently, the donor and acceptor can be expected to be coherently coupled to many of the same vibrations in the medium. As outlined by Hopfield[53], the Förster-Dexter formalism is valid only when the electron transfer process is dominated by the contribution of high-frequency molecular modes.

Finally, the theory has not been completely tested, since in the Chance and DeVault experiment neither the separation between sites, nor the exact nature and redox potential of the sites is known.

3. The Purely Quantum Formulation

Using a formalism analogous to Hopfield's work, Jortner formulated the problem of biological electron transfer in terms of a nonadiabatic multiphonon non-radiative decay process in a dense medium[54].

The resulting rate equation is given by:

$$W_{ab} = A \exp[-S(2\bar{\nu} + 1)] \times I_p \{2S[\bar{\nu}(\bar{\nu} + 1)]^{1/2}\} [(\bar{\nu} + 1)/\bar{\nu}]^{p/2} \quad (13)$$

where

$A = 2\pi |V^2|/\hbar^2 \omega$ with V $(cm^{-1}) = 10^5 \exp(-R)$

R = center-center distance $\mathring{A}$

I_p is the modified Bessel function of order p.

$S = (\Delta^2)/2$ where Δ is the horizontal displacement of the potential minima.

$\bar{\nu}$ is the Bose factor, given by $\bar{\nu} = [\exp(\hbar\omega/KT) - 1]^{-1}$

$p = |\Delta E| / \hbar\omega$

The wavefunction overlap V, expressed in the prefactor A, shows an exponential decrease of the rate with distance increase. There is no significant dependence of A on ΔE, but ΔE does affect P. The mean frequency $<\omega>$ is used to characterize the intramolecular reorganization modes, in the same way as $<\omega_s>$ characterizes the low-frequency medium reorganization modes. For fluid, polar solvents, the polarization modes are of very low energy at room temperature with $KT >> \hbar\omega$, and this fully quantum-mechanical theory reduces to the classical Marcus expression.

A similar equation has been developed by Huang and Rhys[11] to describe the shape of optical absorption bands of F-centres in crystals. They differ only in some constants

having to do with the difference between optical absorption and electron transfer. Further development was achieved independently by Kubo [58] and Lax [9], to obtain much more general cases, including a variety of oscillator frequencies, with changes of frequency considered as well as the changes of equilibrium position, using generating functions as a method of calculation [8,59].

A careful analysis of equation (12), shows that it is useful in describing ET phenomena throughout the entire temperature range exhibiting a continuous transition from temperature independent tunneling between nuclear potential surfaces at low temperatures to a classical activation energy at high temperature. It provides three distinct limiting situations of interest.

a) Extremely low temperature limit, for $kT < \hbar < \omega_s > << \hbar <\omega>$. Since no high energy modes are populated, the physical situation corresponds to temperature independent (nuclear) tunneling occurring from the zero point of the reactant well to any accessible state on the product surface which are nearly degenerate with it.

b) Intermediate limit or thermal excitation of the medium phonon modes, for $\hbar < \omega_s > << kT << \hbar <\omega>$. Now the tunneling occurs from the thermally excited medium phonon modes. It is interesting to note that the rate is temperature-independent. Here the system tunnels through the barrier, corresponding to reorganization of a high frequency mode, while the reorganization of the low-frequency mode occurs classically, providing an apparent activation energy for the system. Levich [5] was the first to point out that the reorganization of the low-frequency polar solvent modes results in a temperature dependent activation energy.

c) High temperature limit, for $\hbar < \omega_s > \ll \hbar \ll\omega\gg \ll KT$. Here the rate of ET is totally temperature dependent, with the activation energy being described by the classical Marcus expression.

The model presented by Jortner, proved to work quite reasonably in the fit of data obtained by DeVault and Chance [25]. The data fit well with $\Delta E = 0.1\,Y$, $\hbar \ll\omega\gg = 400\ cm^{-1}$, $S = 20$, and $A = 10.$[9]

4. Redox Properties of Excited States and Photoinduced electron Transfer Reactions

4-1) Redox Properties of Excited States

Electron transfer has been accepted as a mechanism for deactivation of fluorescence and phosphorescence for many years. After absorption of a photon, the molecule is promoted up to one of its excited states, becoming both a stronger reductant and a stronger oxidant than the corresponding ground state. Here the electron in its excited state is more weakly bound (strong reductant) and at the same time generates an electron hole pair with a hole in a lower level (strong oxidant).

The energy changes for the excitation and ionization process D^*/D^- and D/D^- (or D^+/D^* and D^+/D), where D is the ground-state molecule and D^* is the lowest excited-state molecule are shown in Figure 4, where the oxidation of a porphyrin molecule is described. The electrochemical redox potentials of the couples D/D^+, D^*/D^+ vs. a reference couple A/A^- are related to the free energy changes according to the folowing equation:

$$\Delta G = \Delta H - T \Delta S = -nFE. \tag{14}$$

Assuming that the Stokes shift between ground state absorption and excited state emission is small, the consequently negligible changes in size, shape, and dipole moment in the excited state yields $\Delta S \approx 0$; therefore, the expression acquires a new form:

$$\Delta G = \Delta H \tag{15}$$

Since $\Delta G = -nFE$ and making $nF = 1$, the D^+/D^* (D^*/D^-) redox couple can be

Figure 4. Potential Surface for the excitation and ionization processes of porphyrin. ^1P = ground state porphyrin; $^1P^*$ = lowest singlet excited state; $^3P^*$ = lowest triplet state; P^+ = cation radical

Potential Energy

Nuclear Configuration

evaluated as:

$$E^o(D^+/D^*) = E^o(D^+/D) - E_{0-0}(D \rightarrow D^*)$$ (16)
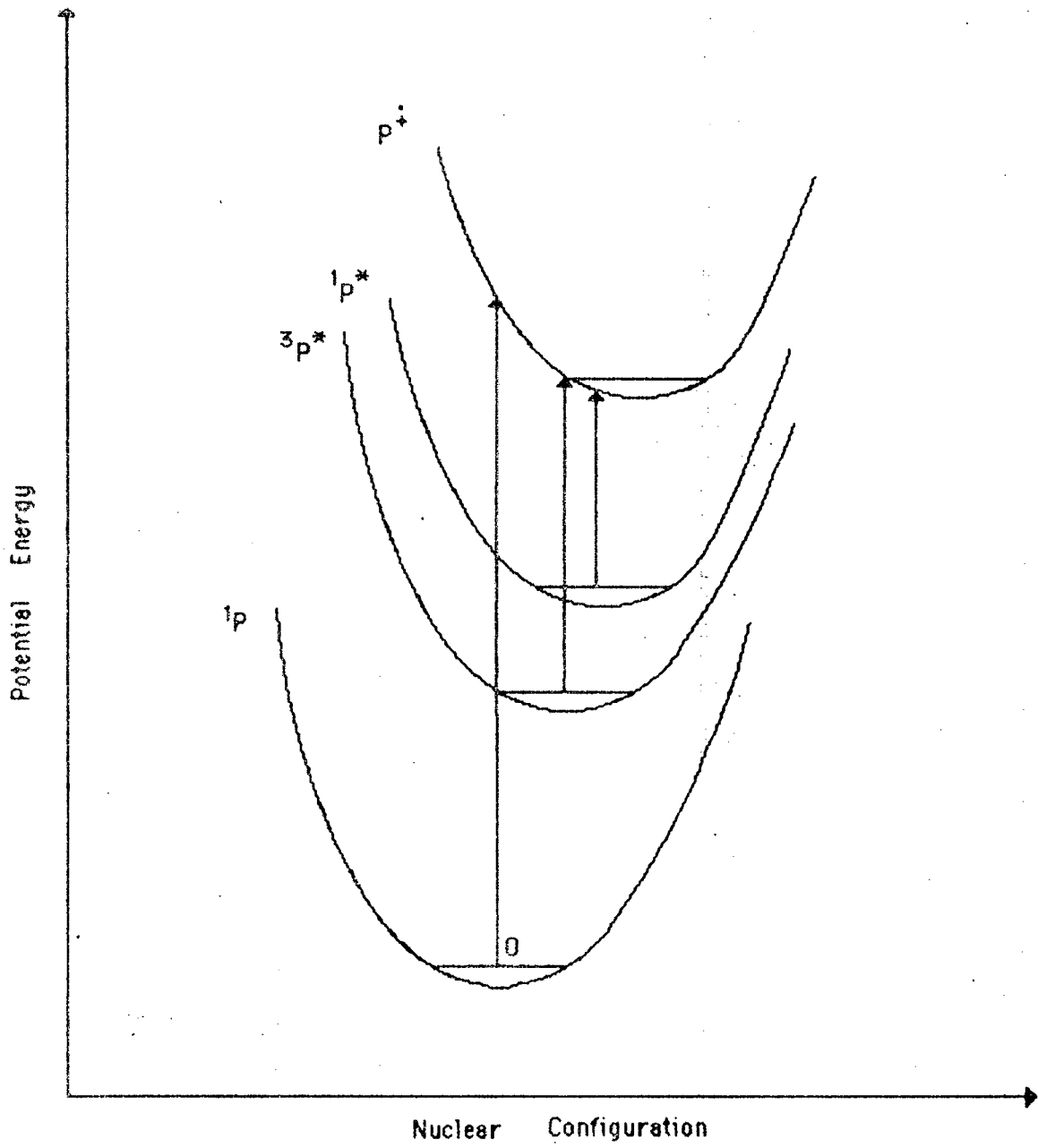
$$E^o(D^*/D^-) = E^o(D/D^-) + E_{0-0}(D \rightarrow D^*)$$ (17)

The values of the excited state redox potential for the transition metal-complexes with bipyridyl and phenanthroiine ligands have been sucessfully predicted from a knowledge of the spectroscopic excited-state energies $E_{0-0}(D \rightarrow D^*)$ and the ground-state redox potentials as described by eq (15) and (16) [43,60,61]. The spectroscopic excited-state $E_{0-0}(P \rightarrow P^*)$ and the ground-state redox properties for several porphyrins derivatives are known and the same calculations are seen to hold [62-64].

A collection of estimated spectroscopic energies and redox potentials for the singlet and triplet excited states for several porphyrin derivatives is available in the literature and is shown in table I and II. The increasing redox potential for both the triplet and singlet excited states of free base tetraphenylporphyrin (H_2TPP) can be envisaged in figure 5. It is clear from here that photoexcitation increases the redox power of H_2TPP by 1.91 V for singlet excited state and by 1.44 V for triplet excited state.

4-2) Photoelectron transfer processes

There are two major processes by which the lowest excited state of a molecule can deactivate in a bimolecular process: energy transfer and electron transfer. These

TABLE I. Estimated Energies and Redox Potentials for the Ground and Singlet Excited States of Porphyrins[a]

porphyrin	Singlet E_{o-o} S-S / eV	$E(P^+/P)$ / V	$E(P/P^-)$ / V	Singlet	
				$E(P^+/^1P^*)$ / V	$E(^1P^*/P^-)$ / V
H_2TPP^b	1.91	1.24	-0.86	-0.67	1.05
$ZnTPPS^c$	2.05	0.86	-1.16	-1.19	0.89
$ZnTPPC^d$	2.03	0.80	-1.25	-1.23	0.78
ZnTPP	2.06	1.04	-1.11	-1.02	0.95
$ZnTMPyP^e$	1.98	1.18	-0.85	-0.80	1.13
PdTPPS	2.21	1.18	-1.04	-1.03	1.17
PdTPP	2.21	1.24	-0.91	-0.97	1.30
PdTMPyP	2.18	1.40	-0.63	-0.78	1.55

[a] Data for pophyrins derivatives are based on ref 70. $E_{1/2}$ values vs. SCE in CH_2Cl_2 from literature have been converted to values vs. NHE by adding 0.24 V. [b] TPP = tetraphenylporphyrin, [c] TPPS = tetrakis(sulfonatophenyl)porphyrin, [d] TPPC = tetrakis (carboxypheny)porphyrin, [e] TMPyP = tetrakis(N-methylpyridyl) porphyrin

TABLE II. Estimated Energies and Redox Potentials for the Ground and Triplet Excited States of Porphyrins

porphyrin	triplet E_{o-o} T-T / eV	$E(P^+/P)$ / V	$E(P/P^-)$ / V	triplet	
				$E(P^+/{}^3P^*)$ / V	$E({}^3P^*/P^-)$ / V
H$_2$TPP	1.44	1.24	-0.86	-0.20	0.58
ZnTPPS	1.61	0.86	-1.16	-0.75	0.45
ZnTPPC	1.60	0.80	-1.25	-0.80	0.35
ZnTPP	1.59	1.04	-1.11	-0.55	0.48
ZnTMPyP	1.63	1.18	-0.85	-0.45	0.78
PdTPPS	1.78	1.18	-1.04	-0.60	0.74
PdTPP	1.80	1.24	-0.91	-0.56	0.89
PdTMPyP	1.81	1.40	-0.63	-0.41	1.18

Data for pophyrins derivatives are based on ref 70. $E_{1/2}$ values vs. SCE in CH$_2$Cl$_2$ from literature have been converted to values vs. NHE by adding 0.24 V.

Figure 5.   Schematic diagram showing the difference in the redox potentials of the lowest excited singlet and triplet state and the ground state of the H_2TPP.

P = H2TPP
E_0 (V)

1.24 — P^+/P

$^1P^*/\overline{P}$ — 1.05

E_{0-0} T-T

0.58 — $^3P^*/\overline{P}$

E_{0-0} S-S

E_{0-0} S-S   0 — NHE

E_{0-0} T-T

−0.20 — $P^+/^3P^*$

$P^+/^1P^*$ — −0.67

−0.86 — $P/\overline{P}$

$E_{0-0}^{S-S} = 1.91$ eV

$E_{0-0}^{T-T} = 1.44$ eV

two quenching processes are often difficult to distinguish since the energy - transfer reactions can lead to the same oxidized or reduced products expected from electron-transfer reactions, and electron - transfer reactions may undergo subsequent reactions, resulting in no net redox chemistry[65]. The ability of an excited state to be involved in an energy transfer process is related to the excited state energy, whereas the ability of an excited state to be involved in an electron transfer process is related to the excited state reduction and oxidation potentials. The nature of the quencher plays an important role in assigning the operative quenching mode. The nature of the quenching mechanism, can be distinguished by knowing the energy of the lowest excited state of the quencher, the ground state redox potential, and the excited state energy of the donor.

Correlations between the quenching rate constants, and the thermodynamic quantities involved for homologous classes of donors and/or quenchers have proved to be useful in the elucidation of the nature of the quenching mechanism. For an electron transfer process the quenching constant increases as the exothermicity of reaction increases, finally reaching a diffusion controlled plateau. Recently Barboy and Feitelson[66] reported the results of the singlet excited-state quenching of zinc octaethylpophyrin (ZnOEP) with a series of quenchers which spanned a large range of redox potentials. They assigned the quenching process as being by electron transfer. The possibility of quenching by energy transfer is ruled out since the lowest excited state of these quenchers lie at higher energy relative to the lowest excited state of the ZnOEP. The plots of log k_q vs standard free energy change ($\Delta G°$) (Fig 6) show that the quenching of ZnOEP follows the reduction and oxidation potential of quenchers known to be electron acceptor and donors, respectively, in a way which suggests that the electron transfer might be responsible for the observed correlation. For good quenchers, in which the

two quenching processes are often difficult to distinguish since the energy – transfer reactions can lead to the same oxidized or reduced products expected from electron-transfer reactions, and electron – transfer reactions may undergo subsequent reactions, resulting in no net redox chemistry[65]. The ability of an excited state to be involved in an energy transfer process is related to the excited state energy, whereas the ability of an excited state to be involved in an electron transfer process is related to the excited state reduction and oxidation potentials. The nature of the quencher plays an important role in assigning the operative quenching mode. The nature of the quenching mechanism, can be distinguished by knowing the energy of the lowest excited state of the quencher, the ground state redox potential, and the excited state energy of the donor.

Correlations between the quenching rate constants, and the thermodynamic quantities involved for homologous classes of donors and/or quenchers have proved to be useful in the elucidation of the nature of the quenching mechanism. For an electron transfer process the quenching constant increases as the exothermicity of reaction increases, finally reaching a diffusion controlled plateau. Recently Barboy and Feitelson[66] reported the results of the singlet excited-state quenching of zinc octaethylporphyrin (ZnOEP) with a series of quenchers which spanned a large range of redox potentials. They assigned the quenching process as being by electron transfer. The possibility of quenching by energy transfer is ruled out since the lowest excited state of these quenchers lies at higher energy relative to the lowest excited state of the ZnOEP. The plots of log k_q vs standard free energy change (ΔG°) (Fig 6) show that the quenching of ZnOEP follows the reduction and oxidation potential of quenchers known to be electron acceptor and donors, respectively, in a way which suggests that the electron transfer might be responsible for the observed correlation. For good quenchers, in which the

Figure 6.   Dependence of rate constant k_q for ZnOEP fluorescence quenching by electron acceptors ($\triangle$, $\blacktriangle$) and donors ($\bigcirc$, $\oplus$). The open and filled symbols refer to acetonitrile and toluene solutions respectively. This figure is adapted from reference **66**
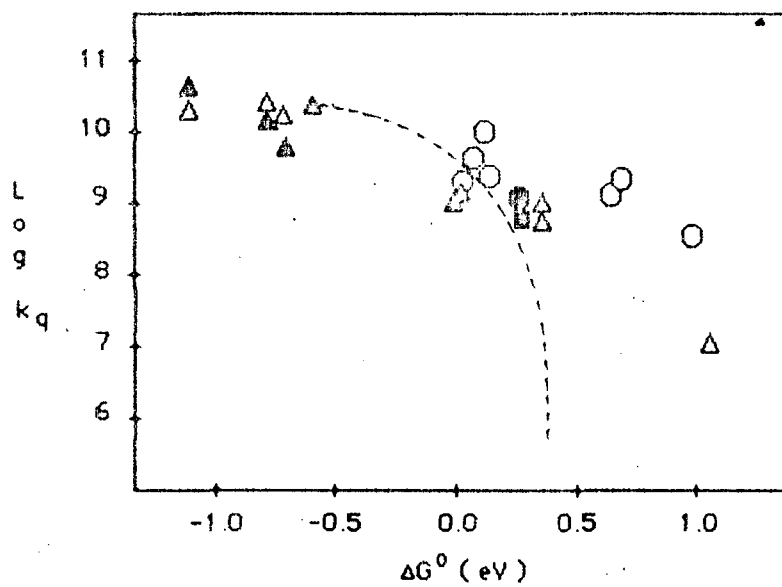
ΔG° of the system is strongly negative, the rate constant is diffusion limited with $K_q = 1.5 \times 10^{10}$ M^{-1} s^{-1}. The broken line in Fig 6 is determined accordingly to the modified Marcus theory, proposed by Rehm and Weller [67,68]. This model predicts the absence of the inverted region for high exothermic and subsequent decrease in log k_q with ΔG° for the quenching by electron transfer. Deviation from the theoretical prediction is observed for rate constants less than $k_q \approx 10^9$ M^{-1} s^{-1}, suggesting that other quenching processes exist and are more rapid than the electron transfer itself. More examples of this kind of approach are provided by the literature [69-74].

B) Electron Transfer reactions in Biological Systems

In view of the available three dimensional and electronic structural information about metalloproteins, many recent advances have occured recently in understanding the most simplest ubiquitous process in life; the transfer of an electron from one site to another in a molecule.

Gray and coworkers [75-79] have studied electron transfer reactions between metalloproteins and small molecules. For example, in an early work [76] they reacted cytochrome c (horse heart) with $Fe(EDTA)^{2-}$, $Co(phen)_3^{3+}$, $Ru(NH_3)_6^{2+}$ and $Fe(CN)_6^{3-}$. The rates of electron transfer were compared to theoretical values calculated using the equations of Marcus theory. They found that the rates varied by a factor of about 10^3 for the various reactants in the order $Fe(CN)_6^{3-} > Co(phen)_3^{3+} > Ru(NH_3)_6^{2+} > Fe(EDTA)^{2-}$. The large variation in the observed rates are attributed to differences in the amount of penetration of the protein surface by the metal. Since most of the protein metal sites are protected from reactants in the medium by peptide chains, reaction with these reactants will involve interaction with the blocking residues with some thermodynamic cost. Another factor responsible for such variation is the degree of the π-overlap between redox centers. Ligands which have orbitals of π symetry available facilitate overlap between the redox centers of the proteins.

Using different metalloproteins they also found that the kinetic accessibility relative to $Fe(EDTA)^{-2}$ increases according to the series azurin $\approx$ High potential-iron sulfur

protein (HIPl) < cytochrome c_{551} < cytochrome c (horse heart) < plastocyanin < stellacyanin. This parallels the extent to which the metal is buried in the peptide.

To determine the distances of separation between the protein redox center to a given reagent, Mauk et al.[77] developed an equation for the reaction distance in a protein self-exchange reaction. The equation is valid only for small E_r and may be written

$$Rp = 6.2 - 0.35 \ln (K_{11}^{\infty}) \tag{18}$$

where R_p equals half the intersite distance for protein self-exchange and K_{11}^{∞} is the calculated self-exchange rate, extrapolated to infinite ionic strength. They found a distance of ~ 10 Å between heme and iron for the reaction of cytochrome c with $Fe(CN)_6^{3-}$.

In recent work, Winkler et al.[78] took advantage of the histidine-33 residue of fericytochrome c to bind the metal complex pentaammineruthenium (III). This is the only imidazole group available for binding and is about 15 ± 1 Å from the heme-iron.

They followed the reaction P-Fe(III)-Ru(II) $\longrightarrow$ P-Fe(II)-Ru(III) . Optical excitation induces electron transfer from tris (2,2' - bipyridine) ruthenium (II), which reduces the ruthenium in the modified protein rather than the iron heme which is buried in the interior of the protein. The reaction was monitored by following the optical absorbance of the reduced iron in the more thermodynamically stable P-Fe(II)-Ru(III). They found that the rate of electron transfer occurs with a rate constant $K_{ET} = 2.0 \pm 0.5 \times 10^1$ s^{-1}. Considering the large separation between the reactant centers and the

small exothermicity ($\Delta E \approx 0.11V$) the measured rate is quite rapid. The reaction shows only a small temperature dependence in the range from 0 to 60°C. These facts suggest that the energy barrier to reaction is very small. Kostić et al.[80] investigated long distance electron transfer in ruthenium-modified azurin and also found a temperature-independent rate.

Isied et al.[81] have studied the same system, using a different approach. They reduced the ruthenium in the modified protein by four different radicals generated by pulsed radiolysis. The radicals were derived from formate, isopropanol, tartarate, and pentaerythritol. The different ratios of P-Fe(III)-Ru(II) to P-Fe(II)-Ru(III) are dependent on the steric factors or on the degree to which the radicals are hydrophobic or hydrophilic. The rate of electron transfer is almost constant and ranges from 53 to 65 s^{-1} and has a positive temperature dependence.

Hoffman et al[82] have reported reactions of [Zn, Fe] hybrid hemoglobins which were prepared by replacing one of the two subunits, α or β, with a photoactive zinc (II) protoporphyrin (ZnP) subunit and keeping the other two subunits with the natural photoinert ferriheme [Fe(III)P]. The electron transfer reaction was initiated by optical excitation of ZnP to form ^{3}ZnP, which reduces the ferriheme in the reaction ^{3}ZnP + Fe(III)P $\longrightarrow$ (ZnP$^+$) + Fe(II)P . The kinetics were followed by monitoring the disappearance of the Soret band of the ground - state zinc (II). They reported $K_{ET} = 60 \pm 25$ s^{-1} at a heme edge-to-edge separation of ~ 16 Å. The back-reaction occurs thermally at a much faster rate (> 10^3 s^{-1}) than the initial transfer reaction.

McLendon et al.[83,84] have reported the use of natural protein complexes known to be involved in biological electron transport processes. For example, they prepared photoactive Zn pophyrin derivatives of cyt-c, cyt-b$_5$, and Hb. For ZnHb-Fe(III)cyt b$_5$ complex, they found that the electron transfer occurs from the photo active zinc porphyrin triplet excited state to form reduced Fe(II)cyt b$_5$ with a unimolecular rate constant $K_{ET} = 6 \times 10^3$ s^{-1}. This rapid and efficient electron transfer quenching occurs at a driving force of $\Delta E \approx 1.0$ V with a separation between the physiological redox centers of ca. 10 Å. Particularly promising work comes from the cyt c/ cyt b$_5$ case since the structure of both reactant proteins are known in some detail. For example, it is known that the hemes are oriented in a parallel fashion and they are sepatated at a distance of 10 Å. The driving force in Zn cyt-c-Fe(III)cyt b$_5$ is $\Delta E \approx 1.0$ V. Rates of electron transfer of $\sim 10^6$ s^{-1} were initially reported.

The Photosynthetic Apparatus

Photosynthesis is the process by which green plants and photosynthetic bacteria convert solar energy into chemical energy. The photosynthetic apparatus is also usefull for studies in electron transfer reactions, since several components employed in the electron transport chain can be isolated. Plant photosynthesis involves a more complex apparatus consisting of two photochemically reactive sites, Photosystem I and Photosystem II. It is important to note that Photosystem I is similar to the bacterial process. More information about plant photosynthesis can be found in a series of

excellent reviews[85-89] and will not be discussed here.

The photosynthetic apparatus employed by bacteria is simpler than that employed by plants and the reaction center can be isolated from light-harvesting antenna - chlorophylls, carotenoids, and in some species phycobilins - with relative ease. The basic components of the bacteriochlorophyll reaction center include the light-activated bacteriochlorophyll P - 870, P, which appears to be a dimeric bacteriochlorophyll in which each of the two units is a magnesium dihydrochlorin; a bacteriopheophytin molecule; I, which has been identified as a magnesium-free pheophytin derivative; and one or more cytochromes, C, as secondary electron donors. A subsequent electron acceptor unit consist of two quinone-ferrous ion complexes, Q. [85-91]

The kinetic events in bacteriochorophyll photosynthesis are summarized in Figure 7.

The reduction of the bacteriochlorophyll by the secondary electron donor (step $CP^+ \longrightarrow$ C^+P) has been the focus of early work in many biological systems which exhibit low temperature independent kinetics. [25, 92, 93] The lack of activation energy at low temperature, found in these systems, initially suggested that an electron tunnelling mechanism was operative. However it is known that the electron tunnelling occurs only in the vicinity of the crossing point of the zero order surface and that its behavior does not affect the temperature dependence of the rate. Considering that the electron transfer occurs simultaneously with the nuclear motion and that this nuclear motion controls the temperature dependence of the rate, Levich and Dogonadze [94] and Sutin [34], suggested that nuclear tunelling, rather than electron tunnelling, was responsible for the temperature independence.

C · P · I · A · Q
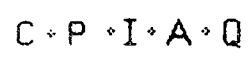
$\downarrow$ Light generates excited singlet state

C · P* · I · A · Q
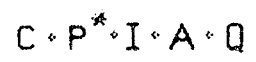
$\downarrow$ Charge separation between $(Bchl)_2$ (P) and BPh (I) creating

           strong oxidant and strong reducant. ~ 10 psec

C · P⁺ · I⁻ · A · Q
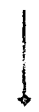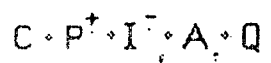
$\downarrow$ Further charge separation; BPh⁻ reduces QFe (A)

           ~ 100 psec

C · P⁺ · I · A⁻ · Q
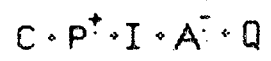
$\downarrow$ $(Bchl)_2^+$ oxidizes cytochrome c (C) , causing further charge

           separation ~ 1 μsec

C⁺ · P · I · A⁻ · Q

$\downarrow$ Primary QFe reduces secondary Q. 50 μsec to 1 msec

C⁺ · P · I · A · Q⁻
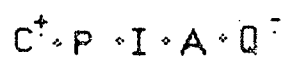
Perhaps the most interesting aspect of photosynthesis is the efficient charge separation which is responsible for the near 100% quantum efficiency of photosynthethic electron transport. After removal or deactivation of the secondary acceptors (quinones) or secondary donors (cytochromes) from the Bacteriochlorophyll system, the long lived charge separation is no longer observed. This has been extensively studied[19,20,22,23,95-97]. The important question here is: how does the photosynthetic system make the back reaction so slow? Different reasons may be suggested for the slow reverse rate of the photosynthetic reaction in vivo including: a) The predicted inverted region, equation (4), is operating: The reverse reactions have a much larger $-\Delta G$ than the forward reactions. The assumption here is that the E_r is the same for both directions and $\Delta G = E_r$ for the forward direction. For the reverse reaction $\Delta G > E_r$, according to equation (4), causes a much reduced reverse rate. Once the protein is isolated from the photosynthetic apparatus, it is free to undergo conformational changes which involve changes in ΔG and E_r. Such changes can result in fast reverse rates. b) Changes in the matrix element $|H_{ab}|$ can be expected after the electron leaves the orbital involved in the forward reaction. Both the orbital and the amount of separation between the reactants might be affected after the forward reaction. Since it is unlikely that the distance between the reactants changes appreciably during the time scale of the kinetic event in a rigid medium, it is more reasonable to accept that the change in $|H_{ab}|$ is due to changes involved in the orbitals after the forward reaction. c) Finally, coupling to specific protein modes plays a part here and was suggested by Sarai.[98,99] These modes

are well-spaced and do not represent a continuum as in homogeneous solution. The forward reaction is facilitated by the matching of the isoenergetic donor-acceptor levels, while the matching may not take place in the reverse direction.

Recently Dutton et al.[100] in an interesting work, observed modification of electron transfer kinetics of reaction centers isolated from Rps. sphaeroides after systematic replacement of the primary endogeneous ubiquinone of photochemical reaction centers with a series of antraquinones (AQ) (Figure 8). This replacement "tunes" properly the driving force of the system. They observed a change in the rate of electron transfer from BPh^- to Q which is a function of the driving force of the system. They also found that at low driving force the endothermic reaction from Q^- to BPh is the major route for electron transfer from Q^- to $(BChl)_2^+$. In the AQ systems, the reduction rate varies from $2 \times 10^4 \ s^{-1}$ for the lowest ΔE to $10 \ s^{-1}$ for the highest ΔE values.

In summary, the biological systems provide powerful experimental vehicles for testing the theories of electron transfer. Nuclear and electron tuneling, efficient charge separation, and both distance and driving force dependence on the rate of electron transfer can be observed and studied by the choice of proper biological systems. The new possibility of manipulating the driving force, the distance, and the orientation of redox partners at will, will open new oportunities to a complete understanding of the problem of electron transfer reactions. To mimic these biological models, parallel work is in progress in synthetic organic and inorganic chemistry which involves the building of molecular models, where the distance, orientation and the energetics can be precisely defined. The information which can be extracted from such systems will be the main subject of the remaining chapters of this work.

Figure 8. A Schematic of the flash induced kinetics and the energy levels of
the redox states of the components of reaction centers isolated
from Rps. sphaeroides. (adapted from ref. 100)

$(Bchl)_2^* BPh\ Q$

$(Bchl^+)_2\ BPh^-\ Q$

$(Bchl^+)_2\ BPh\ Q^-$

$(Bchl)_2\ BPh\ Q$

$2 \times 10^{11} s^{-1}$

$K_1\ 4\times10^9\ s^{-1}$

K_{-1}

$K_2\ 10^8\ s^{-1}$

$K_3\ 10\ s^{-1}$

$h\nu$

Level altered
with quinones
of differing
$E_{1/2}$ values

(Q^-/Q)
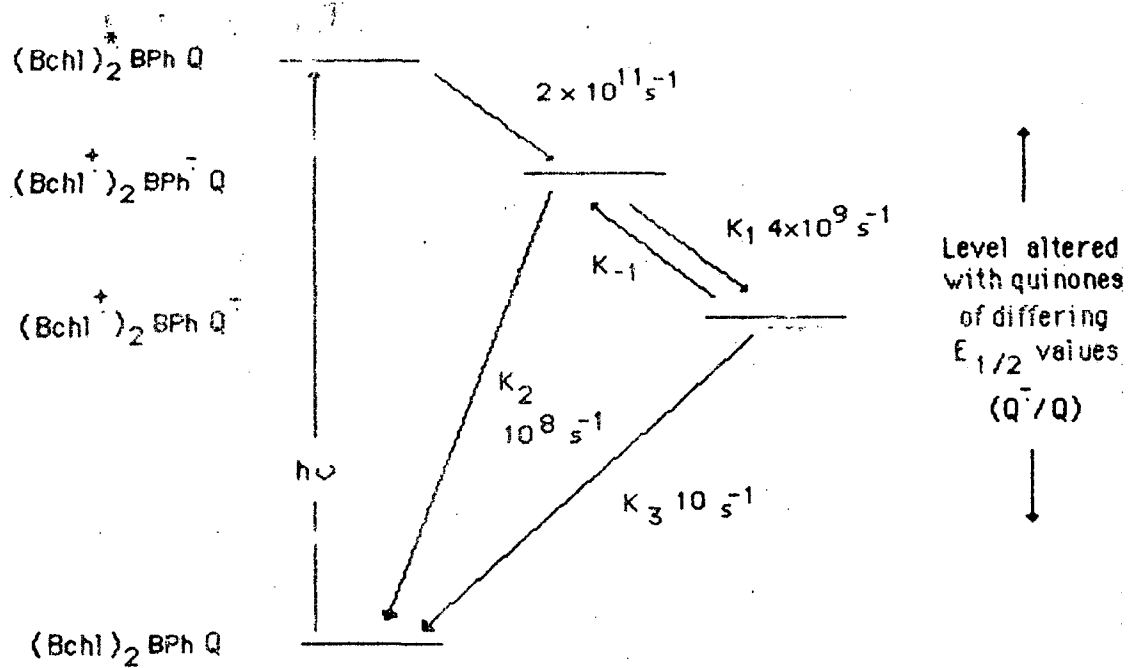
References

1) R. A. Marcus, _Discuss. Faraday Soc._, _29_, 21-31 (1960).

2) R. A. Marcus, _Annu. Rev. Phys. Chem._, _15_, 155-196 (1964).

3) R. A. Marcus, _J. Chem. Phys._, _43_, 679-701 (1965).

4) R. A. Marcus, _Electrochim. Acta_, _13_, 995 (1968).

5) V. G. Levich, _Adv. Electrochem. Eng._, _4_, 249 - 371 (1966).

6) N. S. Hush, _Prog. Inorg. Chem._, _8_, 391 - 444 (1967).

7) N. S. Hush, _Electrochim. Acta_, _13_, 1005 (1968).

8) R. Kubo and Y. Toyozewa, _Prog. Theor. Phys. Osaka_, _13_, 160-182 (1955).

9) M. Lax, _J. Chem. Phys._, _20_, 1752 - 1760 (1952)

11) K. Huang and A. Rhys, _Proc. Phys. Soc. Ser. A_, _204_, 413 (1951).

12) J. Ulstrup and J. Jortner, _J. Chem. Phys._, _63_, 4358 - 4368 (1975).

13) S. Efrima and M. Bixon, _Chem. Phys._, _13_, 447 - 460 (1976).

14) R. P. Van Duyne and S. F. Fischer, _ibid._, _5_, 183 - 197 (1974).

15) N. R. Kestner, J. Logan, and J. Jortner, _J. Phys. Chem._, _78_, 2148 - 2166 (1974).

16) T. Holstein, _Philos. Mag._, _37_, 49-62 (1978).

17) T. Holstein, _Ann. Phys. Leipzig_, _8_, 343 (1959).

18) E. D. German and A. M. Kuznetsov, _Electrochim. Acta._, _26_, 1595-1608 (1981).

19) P. Avouris, K. S. Peters, and P. M. Rentzepis, _Biophys. J._, _21_, 8a Abst M-Am-AI (1978).

20) R. K. Clayton in "Tuneling in Biological Systems", Chance etal. (eds) New York: Academic Press, pp. 377-386 (1979).

21) P. L. Dutton, T. Kihara, J. A. McCray, and J.P. Thornber, _Biochim. Biophys. Acta_, _226_, 81-87 (1971).

22) E.S.P. Hsi and J.R. Bolton, Biochim. Biophys. Acta, 347, 126-133 (1974).

23) J.C. Romijn and J. Amesz, Biochim. Biophys. Acta, 42, 164-173 (1973).

24) D. DeVault, Quart. Rev. Biophys., 13, 387-564 (1980).

25) D. DeVault and B. Chance, Biophys J., 6, 825-847 (1966).

26) T. Kihara and B. Chance, Biochim. Biophys. Acta, 189, 116-124 (1969).

27) M.Y. Okamura, R.A. Isaacson, and G. Feher, Biochim. Biophys. Acta, 546, 394-417 (1979).

28) R.E. Blankenship and W.W. Parson in "Photosynthesis Relation to Model Systems", (ed. J. Barber), pp. 71-114. Amsterdam: Elsevier/North Holland (1979).

29) B. Chance, D. DeVault, H. Frauenfelder, R.A. Marcus, J.R. Schrieffer, and N. Sutin, (eds.) "Tunneling in Biolobical Systems", New York: Academic Press (1979).

30) T.J. Meyer, J. Electrochem. Soc., 131, 221C-228C (1984).

31) I. Imasaka, K. Tanaka, and T. Tanaka, Chem. Lett., 1477-1480 (1983).

32) R. Ziessel, Nouv. J. Chim., 7, 613-633 (1983).

33) M. Julliard and M. Chanon, Chem. Rev., 83, 426-506 (1983).

34) N. Sutin, Ann. Rev. Nucl. Sci., 12, 285-328 (1962).

35) N. Sutin, Acc. Chem. Res., 1, 225-231 (1968).

36) N. Sutin, Acc. Chem. Res., 15, 275-282 (1982).

37) R.D. Cannon, "Electron Transfer Reactions", London: Butterworth (1980).

38) H. Taube, Chem. Rev., 50, 69-126 (1952).

39) S. Fukuzumi, C.L. Wong, J.K. Kochi, J. Am. Chem. Soc., 102, 2928-2939 (1980).

40) J.S. Litter, "Essays on Free Radical Chemistry", Spec. Publ. - Chem. Soc. No. 24, 383-408 (1970).

41) J.S. Litter, MTP Int. Rev. Sci.: Org. Chem., Ser. One, 10, 237 (1973).

42) R.G. Wilkins, "The Study of Kinetics and Mechanism of Reactions of Transition Metals", Allyn and Bacon: Boston, p 252 (1974).

43) V. Balzani, F. Bollete, M. T. Gandolfi, M. Maestri., Top. Curr. Chem., 75, 1 - 64 (1978).

44) J. R. Miller, J. V. Beitz, and R. K. Huddleston, J. Am. Chem. Soc., 106, 5057 - 5068 (1984)

45) R. A. Marcus, J. Chem. Phys., 24, 966 - 978 (1956).

46) R. A. Marcus, J. Chem. Phys. 72, 891 (1968).

47) S. Eherland and H. Gray in Biol. Aspects Inorganic Chem., A. Addison, W. Cullen, D. Dolphin, B. James (eds.), Wiley, N.Y. (1977).

48) R. Marcus, J. Chem. Phys., 38, 1858 - 1862 (1963).

49) D. Holten, M. Windsor, Ann. Rev. Biophys., 7, 189-227 (1978).

50) T. Netzel, P. Rentzepis, J. Leigh, Science 182, 238 - 241 (1973).

51) G. Moore and R. J. P. Williams, Coord. Chem. Revs., 18, 125 - 197 (1976).

52) D. Mauzerall in the Porphyrins V. VI, D. Dolphin (ed.) (1979).

53) J. J. Hopfield, Proc. Natl. Acad. Sci. U.S.A., 71, 3640 - 3644 (1974).

54) J. Jortner, J. Chem. Phys., 64, 4860 - 4867 (1976).

55) T. F. Soules and C. B. Duke, Phys. Rev. B, 3, 262 -274 (1971).

56) T. Förster, Naturwissenschaften, 33, 166 - 175 (1946).

57) D. L. Dexter, J. Chem. Phys., 21, 836 - 850 (1953).

58) R. Kubo, Phys. Rev., 86, 929 - 937 (1952).

59) R. Kubo and H. Kamimura, eds., "Dynamical Process in Solid State Optics", pp. 90 -115, Tokio; Syokabo; New York, Benjamin (1967).

60) N. Sutin and C. Creutz, Pure Appl. Chem., 52, 2717 - 2738 (1980).

61) K. Kalyanasundaram, Coord. Chem. Rev., 46, 159 - 244 (1982).

62) K. Sauer, Acc. Chem. Res., 13, 249 - 256 (1980).

63) M. Calvin, Acc. Chem. Res., 11, 369 - 374 (1978).

64) K. Kalyanasundaram and M. Neumann-Spallart, J. Phys. Chem., 86,

5163 - 5169 (1982).

65) C.T. Lin, W. Bottcher, M. Gov, C. Creutz, and N. Sutin, J. Am. Chem. Soc., 98, 6536 - 6544 (1976).

66) N. Barboy and J. Feitelson, J. Phys. Chem. , 88, 1065 - 1068 (1984).

67) D. Rehm, A. Weller, Ber. Bunsenges. Phys. Chem. , 73, 834 -839 (1969).

68) D. Rehm, A. Weller, Isr. J. Chem. , 8, 259 - 271 (1970).

69) J. N. Domas, J. W. Addington, S. H. Peterson, E. W. Harris, J. Phys. Chem. , 81, 1039 - 1043 (1977).

70) H. E. Toma, C. Creutz, Inorg. Chem., 16, 545 - 550 (1977).

71) A. Juris, M.T. Gandolfi, M. F. Manfrin, V. Balzani, J. Am. Chem. Soc. , 98, 1047 - 1048 (1976).

72) C. Creutz, N. Sutin, Inorg. Chem. , 15, 496 - 499 (1976).

73) A. R. Gutierrez, T. J. Meyer, D. G. Whitten, Mol. Photochem. , 7, 349 - 358 (1976).

74) L. V. Natarajan and R. E. Blankenship, Photochem. Photobiol. , 37, 329 - 336 (1983).

75) S. Wherland and H. B. Gray, in Biological Aspects of Inorganic Chemistry, A. W. Addinson, W. B. R. James, D. Dolphin, Eds., Wiley, New York, 1977, pp. 289-357

76) S. Wherland and H. B. Gray, Proc. Natl. Acad. Sci. U.S.A. , 73, 2950 - 2954 (1976).

77) A. G. Mauk, R. A. Scott, and H. B. Gray, J. Am. Chem. Soc. , 102, 4360 - 4363 (1980).

78) J. R. Winkler, D. G. Nocera, K. M. Yocom, E. Bordignon, and H. B. Gray, J. Am. Chem Soc. , 104, 5798 - 5800 (1982).

79) A. G. Mauk, E. Bordignon, and H. B. Gray, J. Am. Chem. Soc. , 104, 7654-7657 (1982).

80) N. Kostic, R. Margalit, M. C. Che, and H. B. Gray, J. Am. Chem. Soc. , (in press)

81) S. Isied, G. W. Worsila, and S. Atherton, J. Am. Chem. Soc. , 104, 7659 - 7661 (1982).

82) J. L. McGourty, N. Y. Blough, and B. M. Hoffman, J. Am. Chem. Soc. , 105, 4470 - 4472 (1983).

83) G. L. McLendon, J. R. Winkler, D. G. Nocera, M. R. Mauk, A. G. Mauk, H. B. Grey J. Am. Chem. Soc., 107 , 739 - 740 (1985).

84) K. Simolo, G. McLendon, M. Mauk, A. G. Mauk, J. Am. Chem. Soc. , 106 , 5012 - 5013, (1984).

85) K. Sauer , Ann. Revs. Phys. Chem., 30 , 155 - 178 (1979).

86) J. R. Bolton, D. O. Hall, Ann. Rev. of Energy, 4, 353 (1979).

87) J. S. Connolly, in "Photochemical Conversion and Storage of Solar Energy 1982," Part A, J. Rabani, (editor), Weizmann Science Press of Israel, p.174 (1982).

88) J. Fajer, I. Fujita, M. S. Davis, A. Forman, L. K. Hanson, K. M. Smith, Adv. Chem. Ser. , 201 , 489 (1982).

89) P. A. Loach, J. A. Runquist, J. L. Y Kong, T. J. Dannhauser, K. G. Spears, Adv. Chem. Ser. , 201 , 515 (1982).

90) P. A. Loach, D. L. Sekura, Biochemistry , 7, 2642 - 2649 (1968).

91) B. S. Bruce, R. C. Fuller, R. E. Blankenship, Proc. Natl. Acad. Sci. USA , 79 , 6532 (1982).

92) B. Chance and M. Nishimura, Proc. Natl. Acad. Sci. U.S.A. , 46 , 19 - 24 (1960).

93) D. DeVault, J. H. Parkes, and B. Chance, Nature , 215 , 642 - 644 (1967)

94) Y. G. Levich and R. R. Dugonadze, Dokl. Akad. Nauk. SSSR , 124 , 123 - 126 (1959).

95) W. W. Parson, Biochim. Biophys. Acta , 131 , 154-172 (1967)

96) P. A. Loach, M. C. Kung, and B. J. Hales, Ann. N. Y. Acad. Sci. , 244 , 297-319 (1975).

97) J. D. McElroy, D. C. Mauzerall, and G. Feher, Biochim. Biophys. Acta , 333 , 261-277 (1974).

98) A. Sarai, Chem. Phys. Lett. , 63 , 360-366 (1979).

99) S. Sarai, Biochim. Biophys. Acta. , 589 , 71-83 (1980).

100) P. Leslie Dutton, M. R. Gunner, and R. C. Prince in "Trends in Photobiology"
     C. Helene, M. Charier, T. Monteray-Castier, I. G. Laustriat (editors), Plenum,
     New York, pp. 561-570 (1982).

CHAPTER II

Synthesis of Molecular Adducts for Studies in Electron Transfer

INTRODUCTION

In order to test the several competing models for electron transfer, a number of experiments were designed and their results were reported in the literature [1-29]. These experiments involved probing the distance dependance as well as the driving force dependance of electron transfer and they range from electron transfer between two isolated molecules in a rigid matrix to intramolecular electron transfer in a molecule containing both reactant partners. There is also a substantial amount of work involving electron transfer in organized media, such as micelles [1-3], semiconductor solid-liquid interfaces [4], and in monolayer assemblies [5,6] which will not be discussed here.

1. Non-Biomimetic models for electron transfer

A significant amount of work has been done in rigid matrices to probe the distance and driving force dependance of electron transfer. The experimental approach in these works consist of producing trapped electrons by pulse radiolysis of glasses and to monitor the rates of electron tunneling to organic electron acceptors. Since one of the reagents is in excess over the other, its spatial distribution controls the average separation between donor and acceptor. This separation can then be varied systematically by changing the concentration of the reactant which is in excess. It is assumed here that the reactant in excess is randomly distributed in the matrix.

Elegant and highly relevant work was developed by Miller et al [7-10], where detailed studies of electron transfer involving organic molecules in rigid matrices have been performed. This work was then extended to photoinduced electron transfer by other groups [8,11-14]. However, the interpretation of rate data where the reactant is in a

random ensemble is difficult since the acceptors are randomly distributed in the glass, yielding a distribution of transfer rates. Matrix studies are thus of primary value in providing qualitative tests of theory rather than providing the definitive quantitative test.

By holding donor and acceptor redox partners at fixed distances it is possible to surmount the uncertainties associated with the distribution of distances. Using this method, several papers on electron transfer have appeared in which the donor and acceptor are held by a molecular spacer.[15-25]

For example, Taube et al.[15] have prepared some of the best-defined intramolecular electron-transfer models. In Taube's models the redox partners are connected by a bifunctional ligand. The beauty of Taube's models is that the structure of the bridging group can be varied considerably to measure the effects of its electronic structure on the rate of electron transfer. For example, they monitored the rate of electron transfer between cobalt and ruthenium, mediated by 4-4'-Bipyridine and related bridging groups [16]. For the 4-4'-Bipyridine case (shown below)

$$(NH_3)_5 Co^{III}N \bigcirc - \bigcirc NRu^{II}(NH_3)_5$$
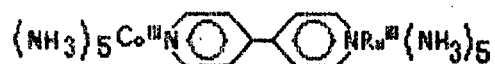
they used an external reducing agent which preferentially attacks the Ru(III) metal, since the reduction of Co (III) involves more reorganization energy. In the next step Ru(II) reduces Co(III) intramolecularly. They assumed that ΔG and the Franck-Condon factors are only slightly affected when the intervening ligand are varied and, therefore, changes in rate can then be attributed to changes in electronic coupling. Using the same strategy but in a more sophisticated way, Stein and Taube [17-18] and Stein and coworkers [19-20] used a series of 2, 3, and 4 ring dithiospiro ligands as bridges

between $Ru(NH_3)_5^{3+}$ and $Ru(NH_3)_6^{2+}$ moieties. They found that the intensity and lineshape of the inter-valence transition are very sensitive to the degree of coupling between the metal centers. The observed decrease in the extinction coefficients reflects a weakening in electronic coupling which was found to correlate well with the number of σ-bonds between metal centers.[20]

In order to more clearly understand the relationship between the bridging ligand structure and the magnitude of the interaction between the metal centers, Richardson and Taube[21] prepared a number of new complexes with the general formula $[(Ru(NH_3)_5)_2 L]^{n+}$ (n = 4, 5, 6), where L is a rigid bifunctional organic ligand. They observed an intervalence band in the near IR for the Ru(II) - L - Ru(III) state for a wide range of ligands. The predicted exponential decrease in the metal-metal interaction with the number of conjugated atoms was observed.[22] However, ligands with an even number of conjugated atoms between metals showed greater metal-metal interaction than those with an odd number.

A number of much more flexibly connected donor and acceptor systems (shown below) have been examined by Hurst et al[23].

$$(H_3N)_5 - Ru^{III} - N\langle\bigcirc\rangle - (CH_2)_n - (HC\!\!=\!\!CH_2) \overset{Cu^I}{\underset{|}{\cdots}}$$
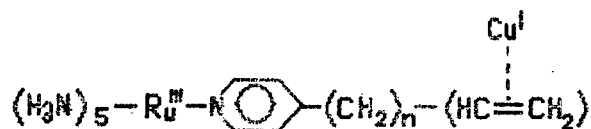
In such a system they observed both thermal and optical electron transfer reactions for n = 0. However, for n = 2, 3, 4, or 7 no intervalence band was observed and the electron transfer rate was second order. Since one might expect the molecule to fold over, an

efficient   pathway   for   electron   transfer   via π- overlap   should   occur.

Verhoeven et al.[24-27] reported more evidence for through-bond interaction from systematic studies on a series of donor/acceptor molecules covalently connected by flexible chain and, more recently, on a series of rigidly connected molecules, some of which are illustrated in Figure 1. They found the presence of an intervalence band in these compounds where the possibility of direct contact between the donor and acceptor groups are minimal. These compounds demonstrate unambiguously that through-bond interactions are more important than through-space interaction.

Miller et al[9] studied   electron transfer in the solid state between two redox sites which were held rigidly apart by virtue of being part of a steroid as shown in Figure 2 A. This figure also shows the separation between donor and acceptor (10 Å). The results are interpreted in light of tunneling theory and qualitative agreement was found between the experimental results and theory. Furthermore Miller and co-workers[28] used the structures of steroids (5 α-androstane), shown in Figure 2B , with a commom electron donor, 4-biphenylyl, and different electron acceptors. The experiments were performed in 2-methyltetrahydrofuran (MTHF) which was frozen to a rigid glass at 77K. At this temperature the donor and acceptor are locked in a fixed conformation. The frozen glass is then subjected to pulses of electrons which causes the ionisation of the solvent giving trapped electrons and radical cations of MTHF. The trapped electrons transfer rapidly to either donor and acceptor with almost statistical probability. Since the electron acceptor has a greater electron affinity than the donor, a nonequilibrium state results.   Photometric absorption measures the rate at which the initial ion distribution reaches equilibrium. These experiments provide direct evidence for very

10 Å

A

$T_{1/2} = < 0.5$ ns $\Delta G^0 = -1.1$ eV

O
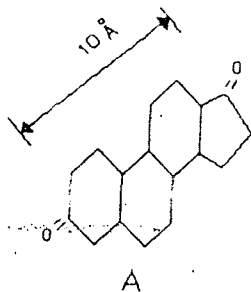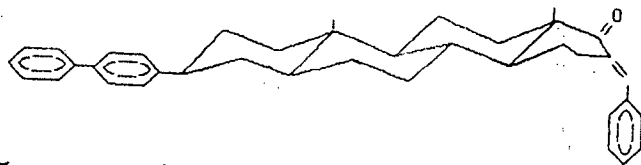
$T_{1/2} = 25$ ns $\Delta G^0 = -0.32$ eV
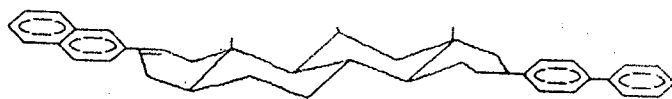
$T_{1/2} = 1$ µs $\Delta G^0 = -0.05$ eV

B

fast electron transfer over a considerable distance (~10 Å). The lifetimes and exothermicities for each system are shown on Figure 2B. The rate of electron transfer in these covalently connected molecules is faster than for equivalent molecules at a comparable separation in glasses, giving some indication that the steroids permit considerable through-bond interaction. This work has been extendend and, in a recent comunication, Miller, Closs and coworkers[29] have reported the synthesis and the kinetic results of a series of eight compounds based on the same steroidal spacer and electron donor described previously. The eight electron acceptor groups were choosen to give an increasing exorthemicity ranging from $-\Delta G = 0.05$ eV to $-\Delta G = 2.40$ eV. Using MTHF as solvent they were able to calculate the major contribution to the total reorganization energy ($\lambda = 1.2$ eV) from the solvent reorganization energy ($\lambda_s = 0.75$ eV) and internal vibrational modes $\lambda_v = 0.45$ eV. According to Marcus theory, the maximum rate should occur for the 2-hexahydronaphthoquininyl where $-\Delta G = 1.23$ eV matches the total reorganization energy λ. Indeed the maximum observed rate constant, 2×10^9 s^{-1} is assigned to 2-hexahydronaphthoquininyl and the rates decreased for higher exothermicity as predicted by the Marcus theory. A plot of $-\Delta G$ vs rate constant is shown on Figure 3. These findings provide the first unambiguous experimental evidence of the 30 year old prediction of the inverted region.

Figure 3. Intramolecular electron-transfer rate constant from biphenyl ions to
(1) 2-naphtyl, (2) 9-phenanthryl, (3) 1-pyrenyl, (4) hexahydro-
naphthoqinon - 2 - yl, (5) 2 -naphthoquinonyl, (6) 2-benzoquinonyl
(7)5-chlorobenzoquinon-5-yl and (8) 5,6-dichlorobenzoquinon-2-yl
in eight bifunctional molecules having the general stuctrure shown
on the figure. This figure is adapated from reference[29].
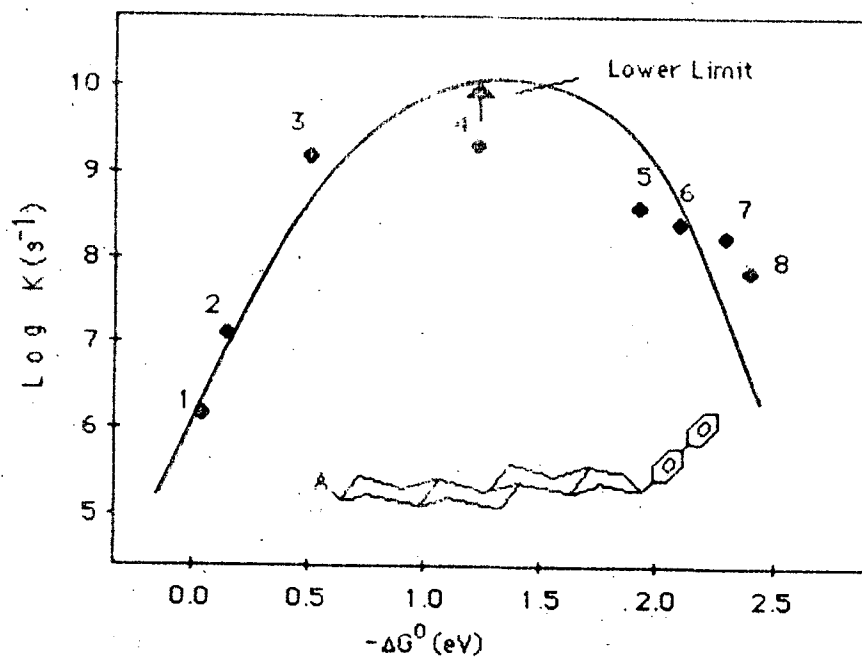
2. Biomimetic models for electron transfer

There have been many attempts to duplicate photosynthesis with artificial systems. In spite of much effort in this area, the progress to date has been slow. The most promising systems recently reported in the literature are the various redox center-linked porphyrins.[30-46], multi-redox centers-linked porphyrins.[39, 47-48] and the doubly linked porhyrins.[49-59] Such systems, when properly designed, can also provide key information on the investigation of the effects of distance, exothermicity and orientation in electron-transfer reactions.

2.1 Various redox center-linked porphyrins system

Kong and Loach [30,31] have reported the synthesis of the covalently-linked porphyrin-quinone complexes with n = 2 and 3 as shown below:
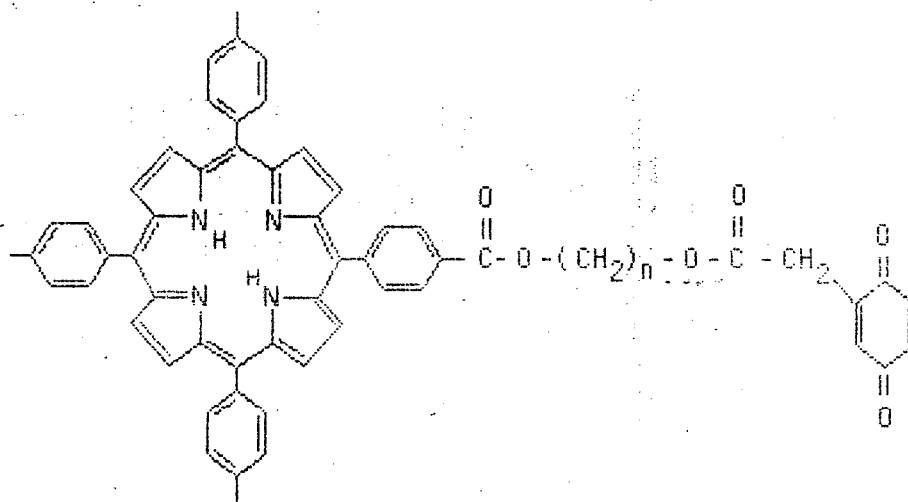
The benzoquinone oxidation state quenches the fluorescence of the attached prophyrin in a variety of organic solvents. They observed a substantial decrease in the fluorescence yield and lifetime in acetonitrile and dichloromethane. Long - lived radicals, generated by an unspecified mechanism, have been detected by electron paramagnetic resonance (EPR).[31] Tabushi at al.[32] reported that the porphyrin fluorescence of the compound shown below is efficiently quenched compared to that of the unlinked porphyrin with an equivalent amount of quinone in solution.
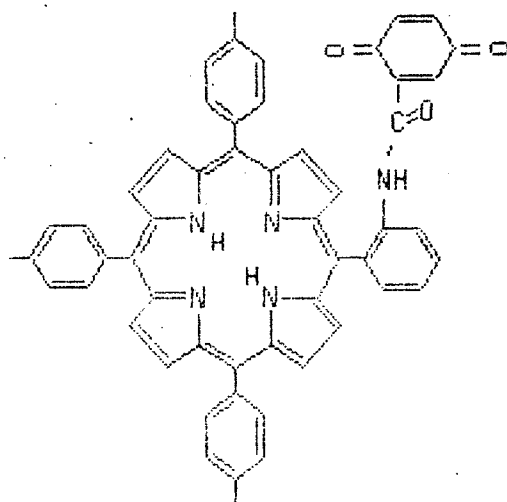
They attributed the fluorescence quenching to electron transfer but presented no direct evidence for such a mechanism. By the use of the same model compound prepared by Kong and Losch, Ho et al.[33] attributed the fluorescence quenching to an intramolecular electron transfer. The photoinduced biradical, $P^{+\cdot} - Q^{-}$, can be detected by EPR. The quantum yield for formation of the EPR signal was very low and other radical-generating reactions, such as electron transfer into the solvent or intermolecular transfer to the quinone moiety of another P-Q molecule could be the cause of the EPR signal rather

than intramolecular charge separation. Further work by the same group[34,35] was done with the porphyrin and a family of quinone derivatives separated by n methylene groups. They found that the short fluorescence lifetime is strongly dependent on the solvent and the specific geometry of the conformers which can have a "complexed" or an "extended" configuration. In the former case the end group is likely to be folded so as to interact with the porphyrin, exhibiting perturbation of the spectra and diminished fluorescence lifetimes and quantum yields, whereas in the late case the porphyrin is relatively unperturbed by the end group. Finally, the light-minus-dark optical difference spectrum produced by irradiation of P-Q molecule in 2-methyltetrahydrofuran at 110 K gives some evidence of a cation porphyrin in the photochemical product complex. They also reported a long lived ion pair product that is stable for hours at low temperature.

Migita et al [36,37] reported the formation of a porphyrin cation radical in the octaethylporphyrin-p-benzoquinone system (OEP) - (CH$_2$)$_n$-BQ (n = 2, 4, 6) upon excitation with a picosecond pulse (30 ps) from a mode-locked ruby laser. They found that the lifetime of the electron transfer state depends upon the length of the methylene chain and the nature of the solvent.

Chidsey and Boxer[38] have prepared a complex which contains a chlorophyll molecule that is covalently connected by a single chain to quinones. The quinones used in this work were chosen so that it would be difficult to reduce them from the triplet excited state. Thus, after the efficient quenching from the singlet excited state, the charge recombination to the triplet state would be sufficiently exothermic to allow triplet formation. They found an efficient quenching of the fluorescence with increasing solvent polarity but no evidence for the formation of a T_0- polarized triplet state by EPR.

Recently, Mataga et al [39] reported the results of the photoinduced electron transfer in (octaethylporphyrin) - $(CH_2)_n$ - (benzoquinone) (PnQ). The observation of an inverse exponential dependence on the length of the intervening methylene chains suggested the possibility of an intramolecular electron-tunnelling mechanism.

A complex with an electron donor and acceptor covalently connected by a flexible chain in a solid solution contains a very large distribution of linked chain conformations, limiting the usefulness of these molecules as a model for testing the distance dependence of electron transfer. In order to overcome this shortcoming, Joran et al [40] have reported the synthesis of three rigid covalently attached side - by - side porphyrin -linker - quinone (PLQ) (Figure 4A) using as spacer units, the bicyclo [2.2.2] octane and bibicyclo [2.2.2] octane which prevent translational displacement and only allow rotational freedom. The edge-to-edge distances are fixed at 6, 10, and 14 Å. They found an indications of a distance dependence from preliminary studies of the static fluorescence quenching of free base PLQ and Zn PLQ systems, relative to a similar porphyrin not linked to a quinone. In another study, Wasielewski et al [41] have reported the synthesis of the porpyrin-quinone shown in Figure 4 B. In these molecules the π electronic system of the porphyrin maintains a minimum 6-7 Å edge-to-edge separation from the quinone, and does not overlap with the π system of the acceptor. The transient absorption spectrum, which was observed 100 ps after the excitation of the ZnTPPNQ system, has been assigned to the $ZnTPP^+NQ^-$ radical ion pair, given an indication that the S_1 depletion is due to electron transfer. Preliminary kinetic results found that photoinduced electron transfer is sensitive to both the exothermicity of the system and the dielectric properties of the medium.

Figure 4. Structure of the rigidly covalently attached quinones reported by Joran et al[40] (A) and Waseielewski et al[41] (B)

A

B

Q =
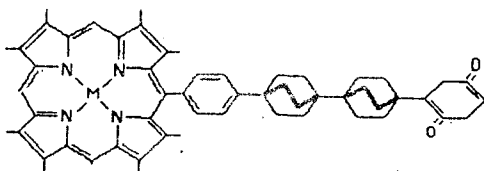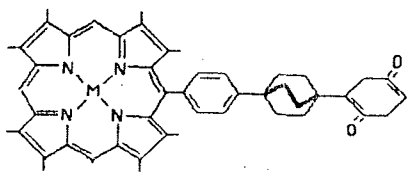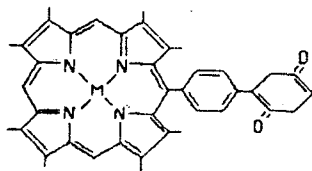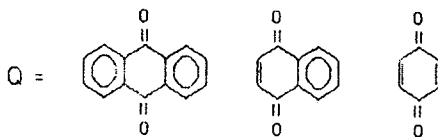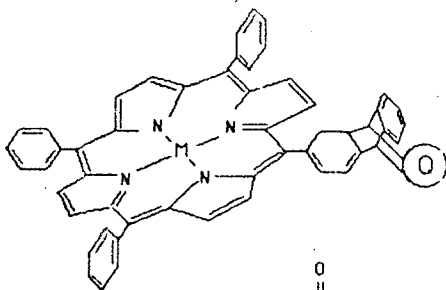
A different approach was adopted by Dalton et al [42] in colaboration with Netzel [43] to overcome the shortcoming caused by the flexible chain linking the porphyrin and their redox counterpart. Instead of using rigid a molecular spacer, they covalently attached benzoquinone directly to the porphyrin at one of the meso positions. The molecule, ϕ_3QP, is shown below:
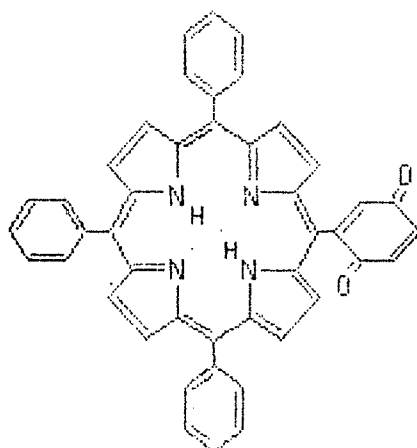
The picosecond transient absorption studies indicated very efficient quenching of the singlet excited state, $\tau < 6$ ps, followed by rapid repopulation of the ground state, along with a substantial triplet yield. The extremely short-lived triplet state, $\tau \approx 30$ ps, generated a triplet ion pair which decayed efficiently to the ground state. The kinetic scheme is shown as follows:

$$\phi_3 QP \xrightarrow{h\nu} [\phi_3 QP]^{S_1} \xrightarrow{0.4} [\phi_3 QP]^{T_1} \xrightarrow{0.1} [\phi_3 Q^- P^+]$$
$$(\tau < 6\ ps) \qquad (\tau = 35\ ps) \qquad (\tau = 10\ ns)$$
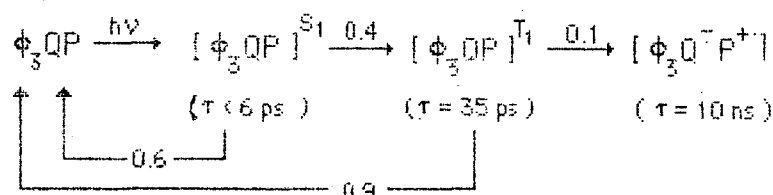
Although the above scheme is kinetically competent, Netzel's work has been

subjected to criticism by Boxer [44] who pointed out the lack of solid experimental evidence for the proposed intermediates and the difficulty of rationalizing the extremely large rates of intersystem crossing from the singlet to the triplet and then from the triplet to the ion pair. Boxer also suggested the possibility of a very large exchange interaction in a singlet ion pair intermediate (not shown), followed by rapid spin-orbit induced triplet-singlet conversion in the ion pair.

Perhaps the most interesting models recently reported in the literature, are the covalently connected cofacial porphyrin-quinones shown in Figure 5. Lindsay et al [45] have prepared a molecule (Figure 5A) containing a porphyrin and a quinone held rigidly at a center-to-center distance of 10 Å. They reported that the fluorescence of the porphyrin is quenched by 60 %. Leighton and Sanders [46] reported the extremely efficient fluroescence quenching caused by the parallel quinone in the model shown in Figure 5 B. This fluorescence quenching is reduced when the intramolecular metal co-ordination forces the quinone to be perpendicular to the porphyrin ring.

Figure 5. The structures of cofacial porphyrin - quinone: (A) multiply covalently connected cofacial porphyrin - quinone reported by Lindsay et al.[45] and (B) porphyrin - quinone covalently conected by single chains reported by Leighton and Sander[46].

A
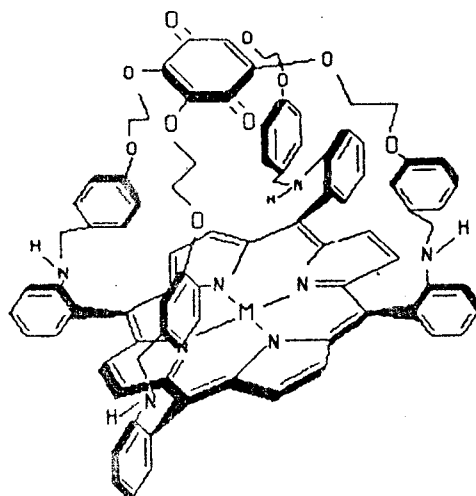
B
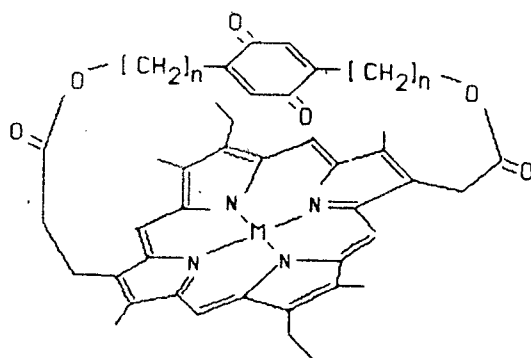
2.2 Efficient charge separation in a multi redox centers-linked porphyrins system.

The most important goal in the artificial photosynthetic conversion of light to other useful forms of energy is to achieve an efficient charge separation. Nature does this very efficiently and several attempts to retard the back-reaction (charge recombination) have been reported. Moore et al.[47], in a series of papers, reported the synthesis of a triad consiting of a porphyrin linked to both a carotenoid and a quinone. This moleule is shown below:
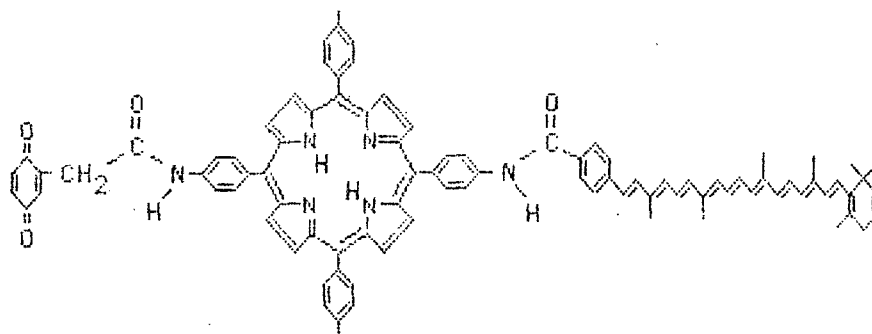
The formation of the transient species $C^{+\cdot} - P - Q^{-}$, occurs in < 100 ps after the excitation of the porphyrin and has a lifetime on the microsecond time scale. This long-lived photodriven charge-separation involves a large redox change.

In another recent work, Mataga et al [39, 48] reported the photoinduced charge-separation process in (etioporphyrin) - $(CH_2)_4$ - (benzoquinone) - $(CH_2)_4$ - (trichlorobenzoquinone) (P4Q 4Q') shown in the following figure. In this system the redox potential of the the two quinones incorporated in P4Q 4Q' are -0.75 and -0.22 V causing a gradient redox potential so as to achieve an efficient charge separation. The picosecond laser photolyses were also done in the P4Q system for comparison.

The synthetic approaches for covalently linked dimeric porphyrins will not be discussed here as a complete review on this subject is available [49].

Kinetically, several works have appeared, but progress in obtaining structurally best-defined systems for studies in ET has been slow. The first initiative in pursuing such systems come from several groups who have prepared cofacial dimeric porphyrins.[50-58] Netzel et al.[56-57] in colaboration with Chang and Boxer and their coworkers[54-55] have reported systematic work concerning the preparation and kinetics of cofacial porphyrins. No photoinduced electron transfer is expected for these compounds, nor for the mixed metal/metal-free ($Mg-H_2$) diporphyrin in non-polar solvent. However, the picosecond optical data from the $Mg-H_2$ diporphyrin in more polar solvents, does show quite different transient absorbance features within 6 ps, in the spectral region expected to contain radical ion absorption. In symmetrical diporphyrins containing either magnesium or free base in both faces, decay occurs instead by a singlet-to-triplet mechanism. The possibility of a very efficient singlet quenching was reinforced by further experiments where quinone added to a solution of the $Mg-H_2$ cofacial porphyrin quenched the primary photoproduct, suggesting that it is an ion pair which reduces the quinone.[58]

Bucks et al.[59] reported the synthesis and kinetics of a series of covalently linked dimers and trimers of chlorophyllide derivatives. The dimers showed no decrease in lifetime or fluorescence quantum yields as ΔG for the system became more negative, ruling out the possibility of electron transfer in the system under study. However, the trimer showed a much more rapid return to the ground state absorbance, suggesting that the triplet yield was low. This fact might be and indication that electron transfer may

be occurring in this trimer, followed by direct recombination to the ground state.

SYNTHESIS OF NON- BIOMIMETIC MODELS FOR STUDIES IN ET

1. Preparation of Intramolecular Electron Donor-Electron Acceptor model based on Diamantane structure

In the search for a good system for testing electron transfer theories we set several criteria in designing appropriate molecular spacers, which are required to hold donor and acceptor redox pairs at fixed distances.

1. The spacers should be conformationally "locked", so that the donor-acceptor distance is unaffected by molecular vibrations or rotations. Optionally, they should also be saturated rings to preclude through bond transfer.

2. The spacer should provide two reactive functional groups to which the donor and acceptor can be linked.

3. The distance between donor and acceptor should vary within a wide range. (ca. 2 - 12 Å).

An ideal system which meets all these criteria is based on diamantane (DAM) shown as follows:
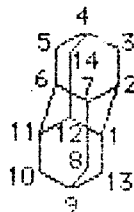
Following the procedure described by Gund and Schleyer [60-61] gram amounts of

diamantane can be prepared from rearrangement of the tetrahydro-derivative of the heptacyclotetradecane "Binor-S" (II) in a cyclohexane solution of $AlBr_3$. "Binor- S" (I), the most readily available of the non-[2+2] dimers of norbornadiene is easily prepared by using $CoBr_2(\phi_3P)_2 + BF_3.OEt_2$ as catalyst. The preparation of diamantane and its precursor are outlined in Figure 6.

This system can be readily and selectively functionalized, providing several possible types of disubstituted derivatives at varying distance of separation. The key reaction for affording such functionalization is the use of specific bromination conditions (ionic vs. Friedel-Crafts) as outlined in the synthetic scheme (Figure 7). The introduction of bromine substituents into the three different positions on the carbon skeleton, forming diapical 4,9-dibromodiamantane (VI), dimedial 1,6-dibromodiamantane (IV) and medial-apical 1,4-dibromodiamantane (V) in varying ratios has been worked out in detail by Gund and Schleyer.[62-64] Because of the bridgehead stereochemistry, elimination, carbocation migration, or other side reactions are precluded.

The aim of this work was to functionalize the diamantane structure in order to obtain the diacid diamantane. The feasibility of this synthesis offers the possibility for the preparation of a wide range of intramolecular electron donor-acceptor systems based on amide or ether linkages for studies on ET reactions. The amide linkage offers an advantage over the ester linkage since it is more stable to hydrolysis than the ester linkage.

Shown below is one example of a simple structure in the present case designed to study the Intervalence Charge Transfer (IVCT).

CoBr$_2$·2PPh$_3$

BF$_3$ OEt$_2$ Δ

(I)

(I)

2H$_2$, PtO$_2$

HOAc , HCl

(96%)

(II)

(II)

Cyclohexane, AlCl3

Δ

(III)
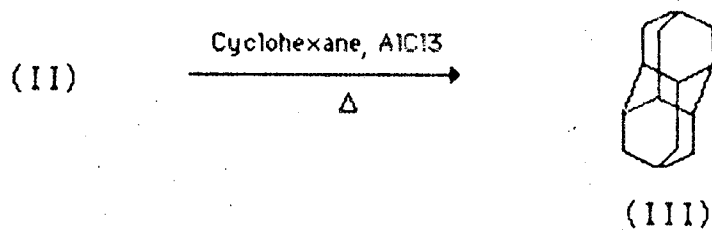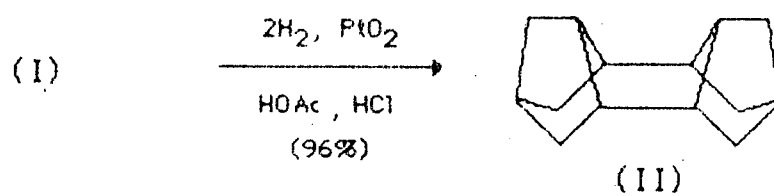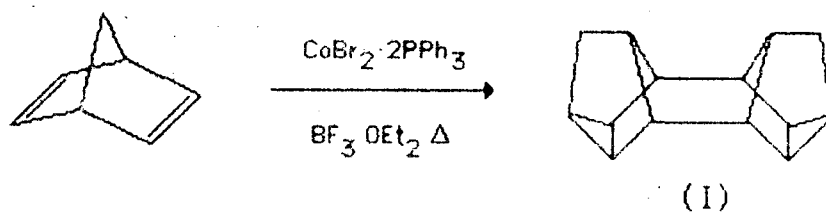
Figure 7 . Selective Bromination of Diamantane

(VII)   (III)

(IV)   (V)   (VI)
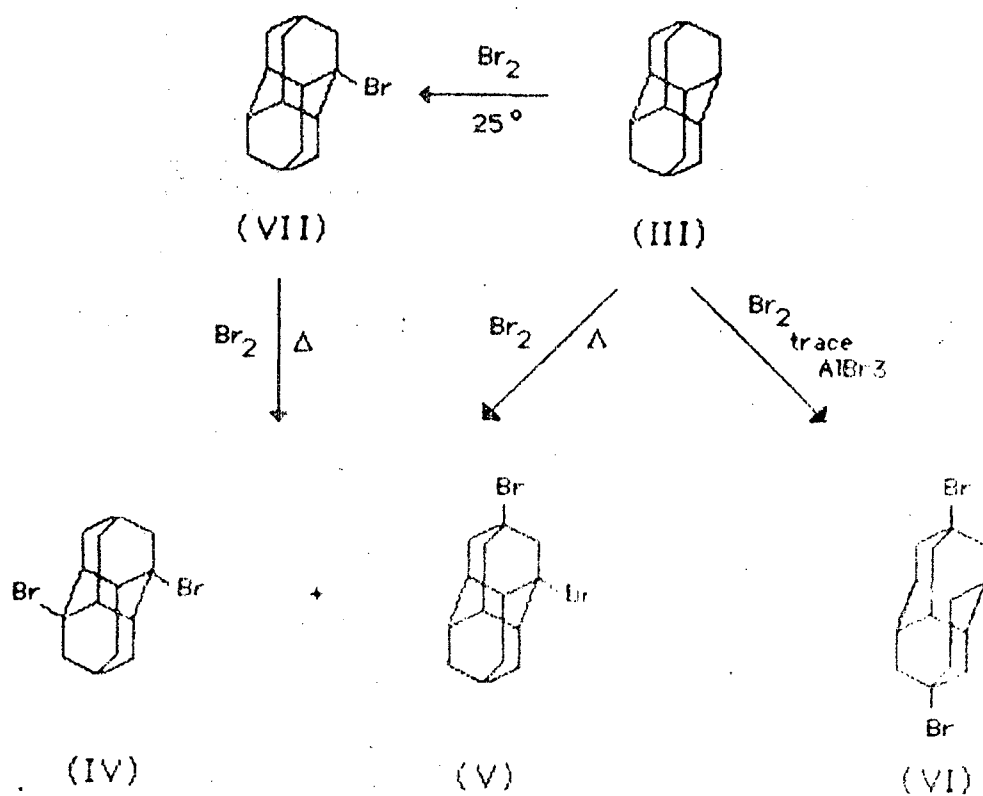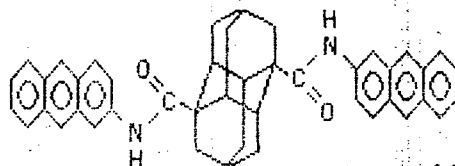
For example, one approach could consist of irradiating a solution of 1,6-dianthracene diamanatane by pulse radiolysis and then monitoring the appearence of the IVCT.

Hush and Miller[65] observed very intense IVCT bands ($\epsilon > 1,000$) when compounds A and B (shown below) were irradiated by pulse radiolysis. Strong interactions

$$\phi_2\text{-}CH_2\text{-}\phi_2$$
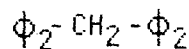
A   B

between redox partners are expected to occur in both systems and the transfer is thought to be through the available p orbital in the bridgehead position in compound A and due to the close proximity of π orbitals in compound B. These interactions are precluded in the diamantane structure: the transfer can only occur through space.

To obtain the dicarboxylic acid diamantane, the Koch-Haaf carboxylation [66-67] method was employed. This approach was used succesfully for substituting adamantane. In the Koch reaction carbon monoxide generated from formic and sulfuric acids captures

a cabonium ion (Eq. 2). In this work, the carbonium ions was generated from tert-butanol, which produced the R^+ through the hydride acceptor $(CH_3)_3C^+$ (Eq. 1).

$$(CH_3)_3C^+ + RH \longrightarrow (CH_3)_3CH + R^+ \qquad (Eq.1)$$

$$R^+ + CO + H_2O \longrightarrow RCOOH + H^+ \qquad (Eq.2)$$
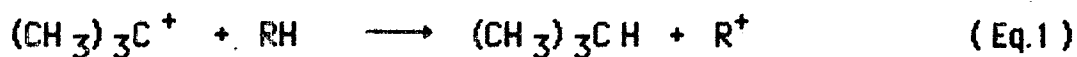
In this way 1,6-dicarboxylic acid diamantane was synthesised and fully characterized. This approach opens new possibilities for further eplications in the preparation of new molecular adducts for studies in electron transfer reaction and solar energy devices.

1.1 Synthesis of dicarboxylic acid diamantane

Synthesis of dicarboxylic acid diamantane, was performed by a series of published procedures. [60-64, 66-67, 78]

<u>Preparation of $CoBr_2.2P\emptyset_3$ catalyst</u>. The precursor, $CoBr_2.2P\emptyset_3$ catalyst was prepared by refluxing overnight 10 g (0.046 mole) of anhydrous cobalt dibromide (Alfa Products) and 24.4 g (0.092 mole) triphenyl phosphine, in 200 ml benzene. After cooling at room temperature, the blue-green catalyst was decanted and dried under vacuum.

<u>Synthesis of Binor-S (1)</u> Two efficient high capacity condensers were attached in series, to a 1-liter, 3-necked flask. The flask was loaded with 200 g of freshly distilled norbornadiene and flushed with N_2. Then, 2.0 g of $CoBr_2.2P\emptyset_3$ catalyst and 5 ml of freshly distilled BF_3 - etherate (Alfa Products) co-catalyst were added and the reaction mixture was heated carefully to ~ 90º C. At this critical point, the heating mantle was removed as soon as the reflux commenced and a vigorous exothermic process took place. This exothermic process was allowed to proceed as rapidly as possilbe and a dry-ice acetone bath was used occasionally as a moderator. (Too much cooling may induce unwanted polymer formation). After cooling to room temperature, 100 ml of methylene chloride was added and the solution was washed with a saturated sodium bicarbonate solution and with water (~ 100 ml). The methylene chloride solution was dried over $MgSO_4$ and evaporated under reduced pressure. The solid was distilled (bp 90º C / ~ 1.5 mm) and gave a white solid, mp 62-63º C (Lit.[78] 63-64º C)

Preparation of Tetrahydro-Binor-S (II)   The catalytic hydrogenation of Binor-S
was performed. 23.6 g of Binor-S (0.078 mole) was partially dissolved in 90 ml of
hot glacial acetic acid containing 10 ml of conc. HCl. Then PtO_2 (0.15 g) catalyst was
added. The mixture was kept under 3 atm hydrogen pressure at 70°C. After three
hours the system was cooled to room temperature. The catalyst was removed by
filtration and water was added causing the appearence of a biphasic solution. The bottom
layer was extracted with methylene chloride, washed with water, dried, and evaporated.
The crude tetrahydro - Binor - S (II) was further purified by distillation under
reduced pressure, bp 105 - 110° C (~ 1.5 mm), to give a colorless and viscous
liquid. NMR ($CDCl_3$) gave a complex spectrum in the range δ 2.25 - 0.75. ^{13}C nmr
(ppm from TMS): Lit.[78] 49.3 (CH)$_2$, 39.0 (CH)$_2$, 37.5 (CH)$_2$, 36.7 (CH)$_2$, 31.9
(CH_2)$_4$ and 27.5 (CH_2)$_2$; Found. 49.7 (CH)$_2$, 39.3 (CH)$_2$, 37.9 (CH)$_2$, 36.9
(CH)$_2$, 32.3 (CH_2)$_4$ and 24.8 (CH_2)$_2$.

Preparation of Diamantane (III).   10 g of Tetrahydro-Binor-S (II) was added from
a dropping funnel to a 100 ml solution of cyclohexane containing 27 g aluminum
bromide. The reaction was initially exothermic but gentle reflux was required after the
addition of tetrahydro-Binor-S. After three hours of reaction time, the cyclohexane layer
was decanted and the catalyst was washed several times with hot cyclohexane until
depletion of diamantane on the catalyst became evident. The combined extracts were then
washed with water and dried over $MgSO_4$. Evaporation of solvent left a semisolid residue
which was partially dissolved in about 100 ml of pentane giving a white solid which
was filtered. The filtrate was further concentrated until diamantane appeared as white
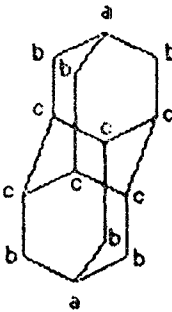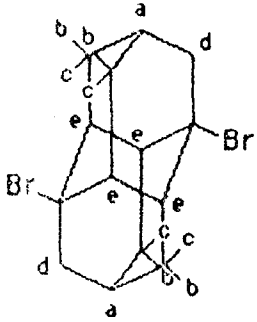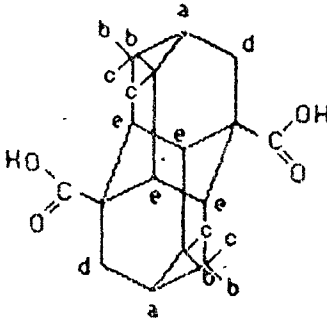
crystals. Recrystallization from pentane gave white crystals, mp 244 - 245 °C (Lit.[78] 244-245). 90 MHz NMR gave a single peak δ 1.68. Better resolution was achieved by the use of 400 MHz as shown in Table II.

Preparation of 1,6 dibromodiamantane (IV). 5 g of diamantane in 25 ml of bromine was heated under reflux overnight. After cooling, the bromine solution was diluted with CCl_4 or $CHCl_3$ and poured onto ice. Small portions of solid sodium bisulfite were then added into the stirring mixture until the bromine disappeared and the solution turned light yellow or colorless. The carbon tetrachloride (or chloroform) solution was then washed with water, dried over $MgSO_4$ and evaporated under reduced pressure. Recrystallization from chloroform gave beautiful white crystals, mp 272 - 274 °C (Lit.[64] 272-273). The 400MHz NMR spectrum and elemental analyses are summarized in Table II.

Preparation of 1,6 Diamantanedicarboxylic acid. Warning! Because carbon monoxide is evolved, the following reaction should be carried out in an efficient hood. A 200 ml three-necked flask with stirrer (vigorous stirrer is required), two dropping funnels and a reflux condenser was charged with 100 ml of cooled H_2SO_4 (conc) and 1.4 g of diamantane in 60 ml of CCl_4. A solution of 20 ml of t-butyl alcohol in 30 ml of HCOOH was then added dropwise over aproximately 1-2 hours . CO evolved vigorously. When the reaction mixture turned pale yellow, the ice bath was removed and the reaction mixture was stirred overnight. The red solution was poured onto crushed ice. The layers were separated and the upper, acid layer was extracted with three 100-ml portions of carbon tetrachloride. The carbon tetrachloride solution was dried over $MgSO_4$

and then evaporated. The material was dissolved in ether and extracted from the ether with a dilute solution of sodium hydroxide. The 1,6-diamantanedicarboxylic acid went into the water layer and was then precipitated by the addition of dilute hydrochloric acid. The crystals which formed were collected by filtration, washed with watter and dried under vacuum. M^+, 277 (276 calcd). The 400MHz NMR spectrum and elemental analyses are summarized in Table II.

TABLE I: [1]H Chemical Shifts of Diamantane and its Derivatives

Compd	Proton Type	area	δ (400 MHz)	Element	Calculated%	Found%
	a	2	1.77			
	c	6	1.72			
	b	12	1.69			
	c	4	2.54	C	48.58	48.47
	d	4	2.50	H	5.24	5.21
	e	4	2.38	Br	46.18	46.39
	a	2	1.98			
	b	4	1.69			
	c	4	1.50 – 1.60	C	69.54	68.45
	d	4		H	7.29	7.72
	e	4				
	a	2	2.06			
	b	4	1.75			

2. Preparation of Intramolecular Electron Donor-Electron Acceptor model based on Porphyrin structure

Meso-tetraarylporphyrins are a totally synthetic family of molecules. Because of their ease of preparation they have been widely used as models for the naturally occurring porphyrins. Since these pophyrins contain a symmetric pattern of substitution, the synthesis involves merely the condensation of four equivalents of pyrrole with four equivalents of aldehyde.[68] The preparation of substituted tetraarylporphyrins by direct substitution of a tetraarylporphyrin is also possible and has been described by Loach et al.[69-70]

Using the mixed aldehyde approach the preparation of the 5-(R), 10, 15, 20 - tritolylporphyrin, where R = 4-pyridyl, is possible. Here the pyridyl group provides a ligand for a second, redox-active metal site on porphyrin and the compound of general structure VIII can be prepared for the study of photoinduced electron transfer.
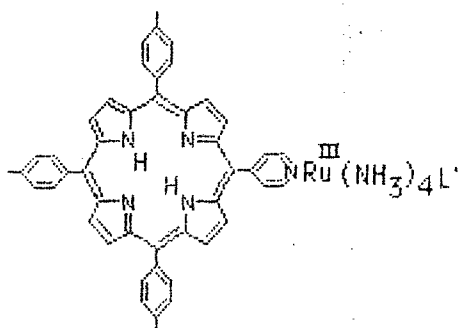
(VIII)

$L = NH_3, Py, 3-Cl-Py$

$M = 2H^+, Zn, Pd$

One of the useful features of VIII for the present study is that the pyridyl groups are constrained out of the plane of the porphyrin ring due to steric interference between the β-pyrrole and o-pyridyl protons.[71] Thus, the overlap between the two π systems is minimized, thereby reducing the adiabaticity of the system. This structural feature is suggested from molecular models (CPK) and X-ray crystallographic structure determinations have generally confirmed this suggestion.[71] Dynamic ^{1}H NMR has been used to estimate the energy barrier for rotation of the phenyl rings in tetraphenyl porphyrin (TPP) metal complexes of Ru (III), In (IIII), and Ti(IV) in which the phenyl rings are unsubstituted or para subtstituted. Since the ortho hydrogens on the two sides of the porphyrin plane are nonequivalent, coalescence of these phenyl proton resonances has been observed, and rotational barriers for these complexes are found to range from 11 to 17 Kcal/mol.[72]

Another feature of the system which makes it attractive for studies on ET is the wide range of driving forces (Table I and II, Chapter I) that can be obtained by replacing the trans ruthenium ligand or the metal in the porphyrin center, and by following the electron transfer from singlet and triplet excited states.

The incorporation of the neighboring ruthenium is performed by following the method of Curtis et al.[73] The synthetic pathway for obtaining different trans ruthenium compounds is described below and was worked out in detail by Isied and Taube [74 - 75] and further improved by Curtis et al.[73]

$[(NH_3)_5 Ru^{III}Cl] Cl_2 + NaHSO_3 \xrightarrow[\Delta]{SO_2} trans-[(NH_3)_4 Ru^{II}(HSO_3)_2]$

$trans-[(NH_3)_4 Ru^{II}(HSO_3)_2] \xrightarrow[\Delta]{HCl} trans-[(SO_2) Ru(NH_3)_4 Cl] Cl$

$trans-[(SO_2) Ru^{II}(NH_3)_4 Cl] Cl + L \longrightarrow trans-[(SO_2) Ru^{II}(NH_3)_4 L] Cl_2$

$trans-[(SO_2) Ru^{II}(NH_3)_4 L] Cl_2 \xrightarrow{H_2O_2/HCl} trans-[(SO_4) Ru^{III}(NH_3)_4 L] Cl_2$

$trans-[(SO_4) Ru^{III}(NH_3)_4 L] Cl_2 \xrightarrow{Zn/Hg} trans-[H_2O Ru^{II}(NH_3)_4 L] Cl_2$

$trans-[H_2O Ru^{II}(NH_3)_4 L] Cl_2 + L' \longrightarrow trans-[L' Ru^{II}(NH_3)_4 L] Cl_2$
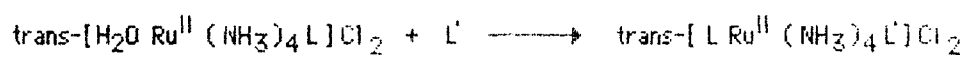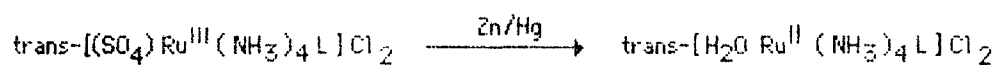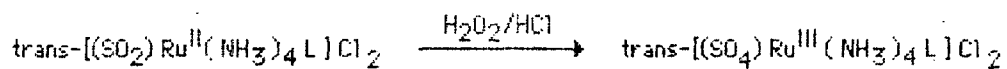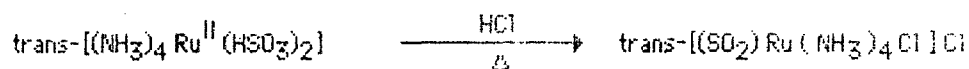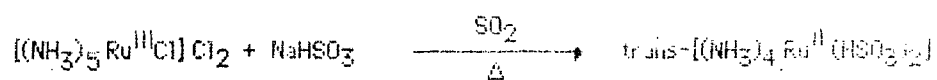
2.1 Synthesis of Bifunctional Porphyrins and their precursors

The free ligand porphyrin , 5 - (4 - Pyridyl) - 10, 15, 20 - tritolyl- porphyrin, was prepared by analogy to the procedure of Little et al.[69] with the use of a mixed aldehyde approach. 4 g of Pyridine-4- carboxaldehyde (Pfaltz & Bauer) and 13 g of p-tolylcarboxaldehyde (Aldrich) were mixed in 500 ml of hot propionic acid (Alfa Products). Ten grams of freshly distilled pyrrole (Aldrich) were then added and the mixture refluxed for one hour. After cooling, the purple crystalline product was collected by filtration and washed with methanol. The crude product was dissolved in chloroform and chromatographed on a 60 X 5 cm column of silica gel (100 mesh, Baker). The second band was further purified by preparative TLC on alumina plates to give 600 mg of analytically pure product. Anal: Calcd (found) for $C_{46}H_{35}N_5.4H_2$ C, 75.7 (75.7); H, 5.9 (6.1); N , 9.6 (9.2). M $^+$, 658.1 (657.9 calcd); strong peaks at $M^+-(C_7H_7)_n$, n = 1, 2, 3. Further purification of the second band was achieved by dissolving the material in reagent grade methylene chloride and rechromatographing on a 40 X 2 cm column of silica gel. The 400 MHz NMR spectrum and the absorbance and emission spectral features of the final product are summarized in tables II and III.

The $[Ru^{III}(NH_3)_5Cl]Cl_2$ was used as the starting material for the synthesis of the bifunctional porphyrins described herein and was synthesized according to the literature method.[79]

The $[Ru^{II}(NH_3)_5H_2O](PF_6)_2$ was prepared according to the procedure published by Curtis et al.[73] with minor modifications. In a typical preparation a 0.1 -g sample

Table II. Absorption Maxima, Extinction Coefficients[a] and Emission Properties of $H_2TPP(P-CH_3)_3(4-Py)$ in DMF solution

absorbtion (extinction coefficients)					fluorescence
Soret	IV	III	II	I	λ_{max}/nm
418 (520.0)	514 (22.0)	549 (10.0)	590 (6.7)	646 (6.0)	654 (2.7)[b], 721 (1.0)

[a] λ_{max}/nm in nm; ϵ in 10^3 $M^{-1}cm^{-1}$. [b] Relative Intensity.

Figure 7. Schematic illustration of the primary photochemistry in bacterial reaction centers

of [$Ru^{II}(NH_3)_5Cl$]Cl_2 was added to a Ag TFA (I) (Trifluroacetic acid) solution which was made by dissolving 0.150 g silver (I) oxide (Fisher Scientifc) in 5 ml of water, with minimum TFA (Aldrich). After filtration the resulting solution of chloropentaammine ruthenium (III) trifluoroacetate was then reduced by reaction with zinc amalgam in a well degassed solution under Argon atmosphere (Air products). The reaction time cannot exceed a period of time longer than 45 min. Upon completion the solution was separated from the zinc amalgam, filtered, and to the filtrate a saturated solution of (NH_4) PF_6 (Alfa Products) was added. This resulted in the immediate precipitation of the pale yellow product which was collected by filtration, washed with ethanol-ether (20 - 80%), and dried under vacuum. Anal. Calcd (found) for [$Ru^{II}(NH_3)_5H_2O$]$(PF_6)_2$ H, 3.47 (3.31); N, 14.11 (13.97)

In a typical preparation, the [$Ru^{III}(NH_3)_5(P)$] $(PF_6)_3$ (P = 5 - (4-Pyridyl) - 10,15,20-tritolylporphyrin) was obtained by dissolving 0.1316 g of [$Ru^{II}(NH_3)_5$ H_2O]$(PF_6)_2$ (10 fold excess) in 50 ml of argon degassed acetone, yielding an orange solution of the [$Ru^{II}(NH_3)_5(CH_3COCH_3)$]$^{2+}$ ion. To this was then added 42.4 mg of P (5-(4-Pyridyl)-10,15,20-tritolylporphyrin). The solution was allowed to stir at room temperature under a blanket of argon for at least 4h. To the reactant medium was added a concentrated aqueous solution of NH_4PF_6. The solid was collected by filtration and washed extensively with water until the red color disappeared from the filtrate solution. The product was washed with ether and dried under vacuum. It was possible to isolate the ruthenium (III) compound by washing the solid extensively with chloroform.

The 400 MHz NMR spectrum is summarized in table III. The elemental analyses for the low yield oxidized product (~ 60 mg) gave the following results; Anal. Calcd (found) for [Ru^{III} (NH$_3$)$_5$ (P)] (PF$_6$)$_3$. 2(CH$_3$)$_2$ CO (P = 5 - (4 - Pyridyl) - 10,15, 20 - tritolylporphyrin) C, 44.8 (45.2); H, 4.48 (4.43); N, 10.0 (10.6); Ru, 7.2 (7.3).

Synthesis of trans-[P Ru^{III} (NH$_3$)$_4$ (L)] (PF$_6$)$_3$ (L = py and 3-Cl-py and P = 5-(4-Pyridyl)-10,15,20-tritolylporphyrin) was performed according to procedures described by Isied and Taube [74-75] with improvements by Curtis et al.[73]

The first step was the synthesis of trans - [SO$_2$ (NH$_3$)$_4$ Ru^{II} Cl] Cl.   2.5 g of [(NH$_3$)$_5$ Ru^{II} Cl] Cl$_2$ was dissolved in a 100 ml of water and heated to 80 °C. Then 3.55 g of NaHSO$_3$ (Alfa Products) was added to the solution and kept for approximately 90 min under a continuous stream of SO$_2$ (Air Products) gas. After cooling, the pale yellow crystals of trans - [(NH$_3$) Ru^{II} (HSO$_3$)$_2$] were collected by filtration, washed with acetone, and dried under vacuum. The crystals were then dissolved in 6M HCl, and heated carefully until the color of the solution turned to orange. The orange crystals were filtered from the cool solution. The trans-[(SO$_2$)Ru^{II} (NH$_3$)$_4$Cl] Cl was recrystallized by dissolving in a minimum volume of hot 0.01 M HCl, and filtering while hot into 25 ml of 1 M HCl. Anal. Calcd (found) for [Ru^{II}(NH$_3$)$_4$(SO$_2$) (Cl)] Cl 2. H$_2$0 H, 3.92 (4.05); N, 18.18 (18.27).

The trans-[SO$_4$ Ru^{III} (NH$_3$)$_4$ (L)] Cl (L = py and 3-Cl-py) was prepared by dissolving 0.1 g of trans-[(SO$_2$) Ru (NH$_3$)$_4$Cl] Cl in 5 ml of neutral H$_2$0 at ~ 40 °C.

A fivefold molar excess of L was added and the color change from orange to yellow. After 15 min of reaction time, the product was precipitated by the addition of 15 volumes of acetone. The suspendend crystals were decanted, washed with acetone and ether, and then dried under vacuum. This solid was then dissolved in 5 ml of double distilled water, filtered, and to the filtrate was slowly added 3 ml of a 1:1 mixture of 30 % H_2O_2 (MCB reagents) and 2 N HCl. After stirring for 10 min, the oxidized product was quenched by the addition of 15 volumes of acetone. The final product was decanted, and dried under vacuum. Anal. Calcd (found) for [$Ru^{III}(NH_3)_4(SO_4)(Py)$] Cl H, 4.51 (4.17); N, 18.44 (18.31).

The [(SO_4) Ru^{II} (NH_3)$_5$ H_2O] (PF_6)$_2$ was prepared following the same method described herein for the synthesis of the [Ru^{II} (NH_3)$_5$ H_2O] (PF_6)$_2$.

The trans-[P $Ru^{III}(NH_3)_4(L)$](PF_6)$_3$(L=py and 3-Cl-py and P=5-(4-Pyridyl) -10,15,20-tritolylporphyrin) were prepared by dissolving trans-[(SO_4) Ru^{II} (NH_3)$_4$ H_2O] (PF_6)$_2$ (10 fold excess) in 50 ml of argon degassed acetone, yielding an orange solution of the trans-[(SO_4) Ru^{II} (NH_3)$_5$ (CH_3COCH_3)]$^{2+}$ ion. To this was then added 42.4 mg of P(5-(4-Pyridyl)-10,15,20-tritolylporphyrin). The solution was allowed to stir at room temperature under a blanket of argon for at least 12h .(More time is required for L = 3-Cl-Py). To the reactant medium was added a concentrated aqueous solution of NH_4PF_6. The work-up was identical to that followed in the synthesis of [Ru^{III} (NH_3)$_5$ (P)] (PF_6)$_3$. Anal. Calcd (found) for : [Ru^{III} (NH_3)$_4$ (P)

(Py)](PF$_6$)$_3$ H, 3.91(4.06); C, 45.68 (45.06); N, 10.44 (10.44) and [Ru^{II}(NH$_3$)$_4$

(P) (3-Cl-Py)] (PF$_6$)$_3$ H, 4.17 (4.12); C, 49.78 (48.67); N, 11.38 (11.21).

All compounds were characterized by cyclic voltammetry. The results are shown in Table IY. These compounds appear to undergo fairly rapid solid-state decomposition; however, reproducible electrochemical and spectroscopic data were obtained as long as the experiments were carried out within several days of their preparation and isolation.

The oxidized adducts [Ru^{III} (NH$_3$)$_5$ (P)] (PF$_6$)$_2$ and trans-[P Ru^{III}(NH$_3$)$_4$(L)] (PF$_6$)$_2$, were generated in situ by the addition of a small amount of bromine vapor to a solution of the compound dissolved in DMF. The ruthenium (II) compounds can also be oxidized and isolated by following the method described by Curtis et al.[73]

Table IV: $E_{1/2}$ Values vs. the NHE in DMF (V).

Compd	$E_{1/2}$ $(Ru^{III/II})$	$E_{1/2}$ $p^{+/0}$
Ru(NH$_3$)$_5$Py	0.40	
Meso H$_2$TPP(pCH$_3$)$_3$(4Py)		1.38
[P Ru(NH$_3$)$_5$] (PF$_6$)$_3$[a]	0.40	1.47
[tr-Ru(NH$_3$)$_4$(Py)$_2$](PF$_6$)$_3$	0.59	
[tr-P Ru(NH$_3$)$_4$Py](PF$_6$)$_3$	0.58	1.43
[tr-PyRu(NH$_3$)$_4$(3-Cl-Py)](PF$_6$)$_3$	0.62	
[tr-PRu(NH$_3$)$_4$(3-Cl-Py)](PF$_6$)$_3$	0.66	1.44

[a] P = Meso-H$_2$TPP(pCH$_3$)$_3$(4PY)
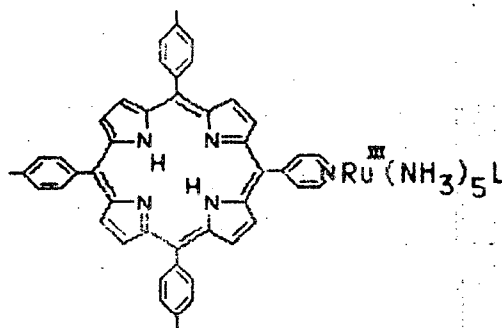
2.2 Results

The synthesis of mono-substituted porphyrin, $H_2TPP(p-CH_3)_3 (4-Py)$, was accomplished by means of a mixed-aldehyde approach. The desired prophyrin crystallized from the reaction mixture along with tetratolylporphyrin and small amounts of polysubstituted totraaryl porphyrins, which were separated by column chromatography. The final product is obtained in low yield. Notice here that the yields of tetra - substituted porphyrins by means of the same approach rarely exceed 25%.[69]

This compound gave satisfactory elemental analyses, when water of crystallization is included. Table II lists the electronic absorption and emission data. The electronic absorbtion spectra are listed with adoption of the numbering system (I-IV) for the visible bands used by Falk.[76]

The aromatic region of the 400-MHZ NMR spectra shown in Fig 8. clearly indicate the structure of the $H_2TPP (p-CH_3)_3 (4-Py)$. The pyrrole, tolyl and pyridyl protons are labeled in Figure 8. A comparison with the spectral patterns obtained from the tetratolyl porphyrin, Figure 9 helps in the assignement of the chemical shifts observed for the pyrrole and tolyl protons. In both, the peaks due to ortho and meta tolyl protons, and pyrrole protons (c) are found in the same region as in the tetratolyl porphyrin spectra. However, the presence of the pyridyl group in one of the meso position of the ring, causes the appearence of two more pyrrole peaks, assigned as a and b. Such effects are widely observed in mono and polysubstitited porphyrins.[77] The integration area for all the peaks support the assigned structure. Mass spectral data (Figure 10) also supports the assigned structure and shows the expected parent peak.

The incorporation of Ru (III) in the pyridyl group was accomplished by the methods

Figure 9. 400 MHz spectra of the aromatic regions of the tetratolylporphyrin
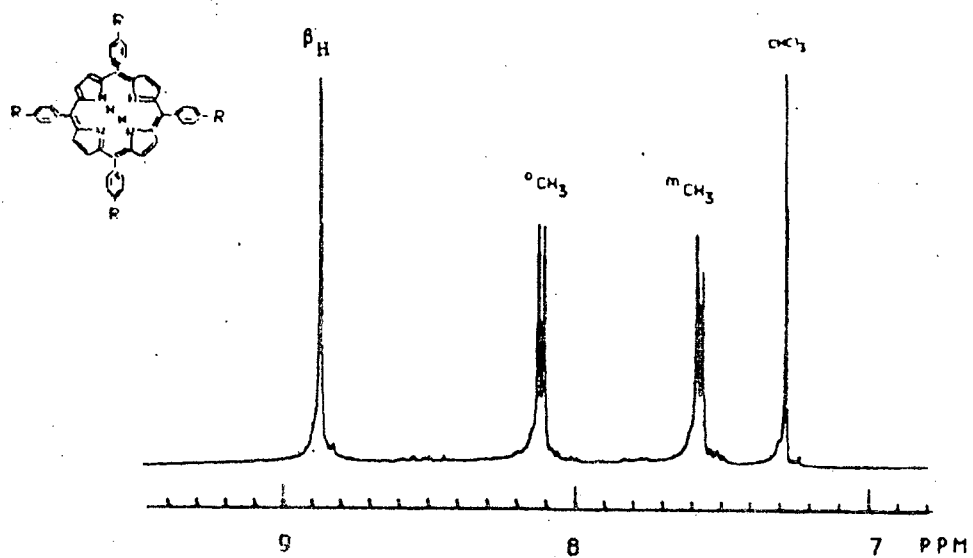
figure 8. 400 MHz spectra of the aromatic regions of the $H_2TPP(p-CH_3)(4-Py)$
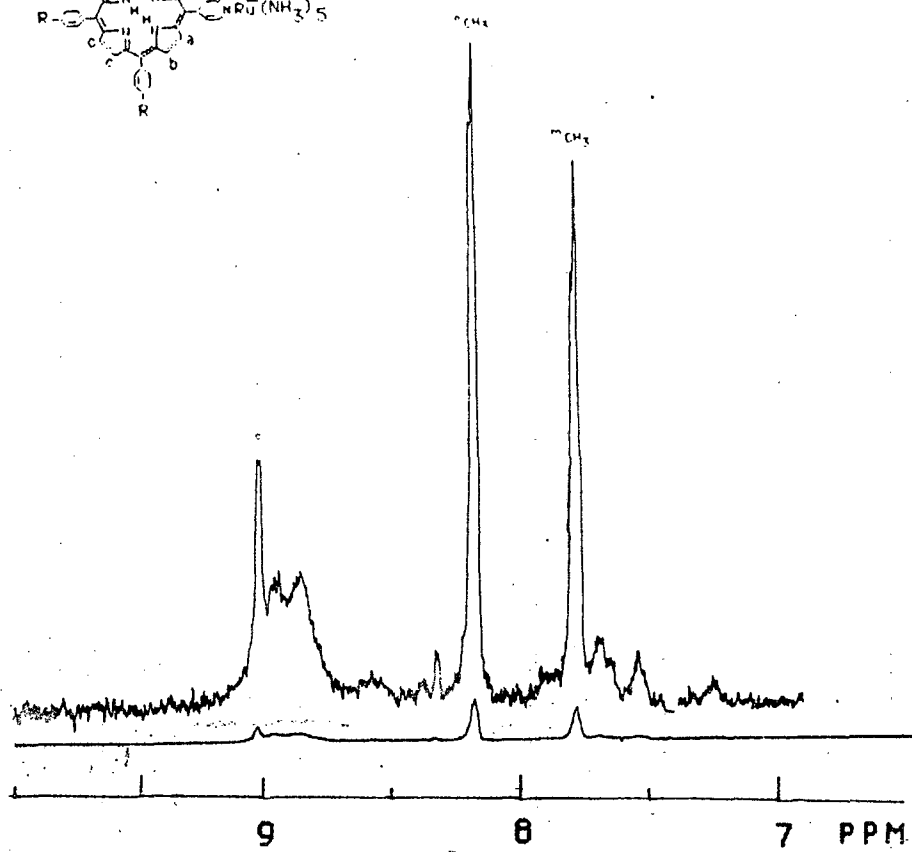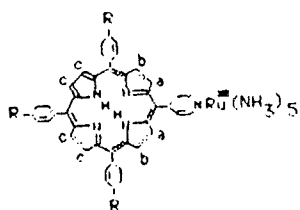
Figure10. Mass spectra of $H_2TPP(p-CH_3)_3(4-P_y)$

Volts vs. Ag/AgCl
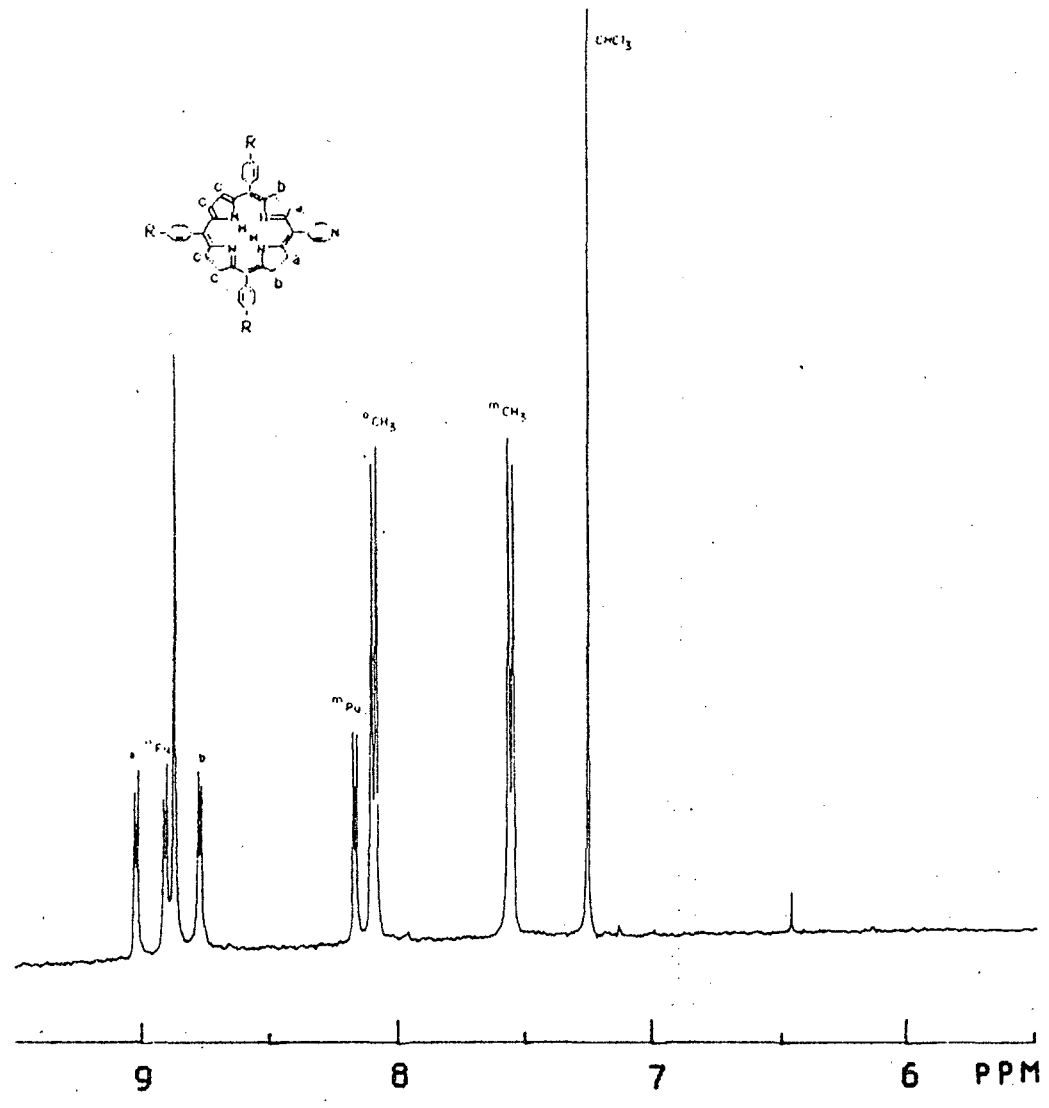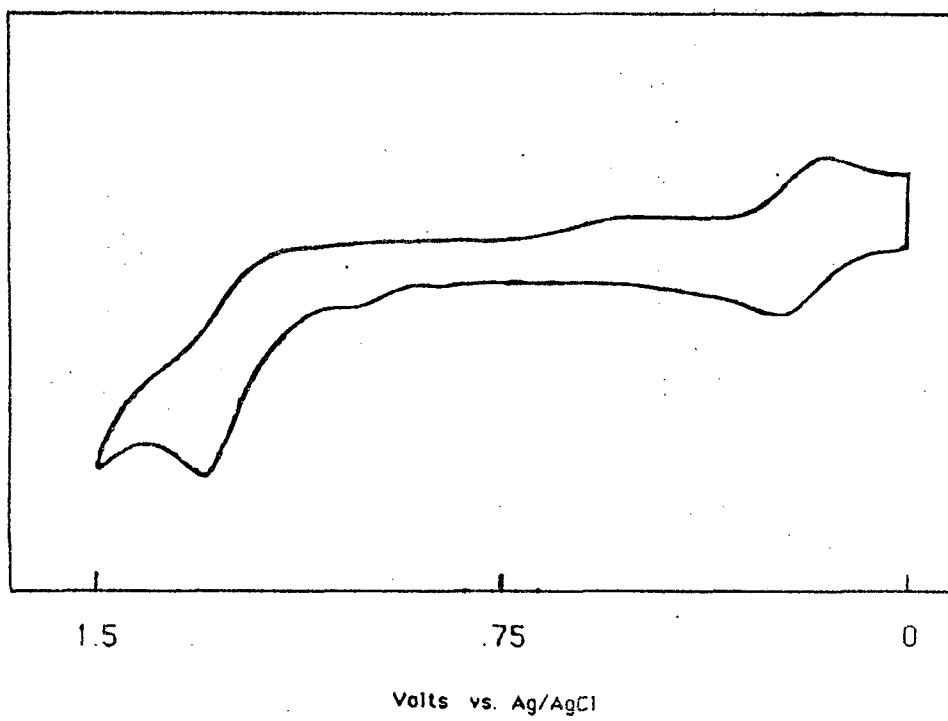
Figure 13. a) Cyclic voltamogram of trans - $H_2TPP(p-CH_3)_3(4-Py)Ru(NH_3)_4Py$

b) Cyclic voltamogram of trans - $H_2TPP(p-CH_3)_3(4-Py)Ru(NH_3)_4(3-Cl-Py)$

a)

i

1.4   .7   0

Volts vs. Ag/AgCl

b)

i

1.4   .7   0

Volts vs. Ag/AgCl
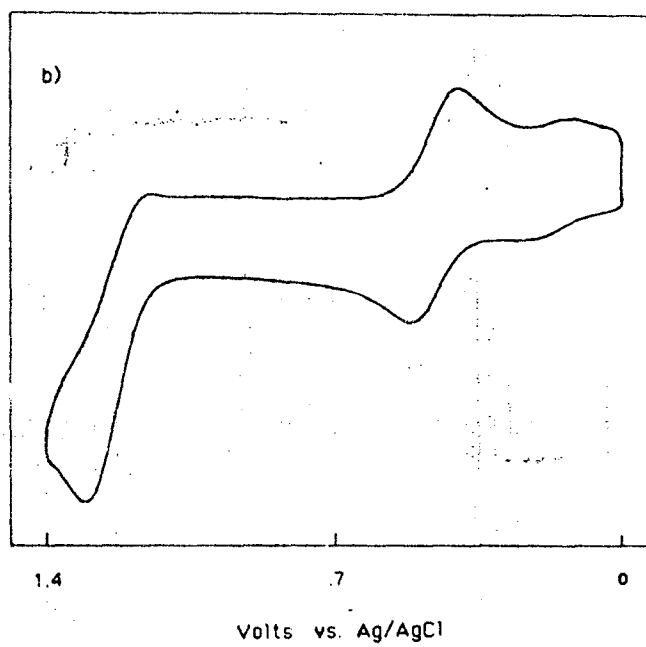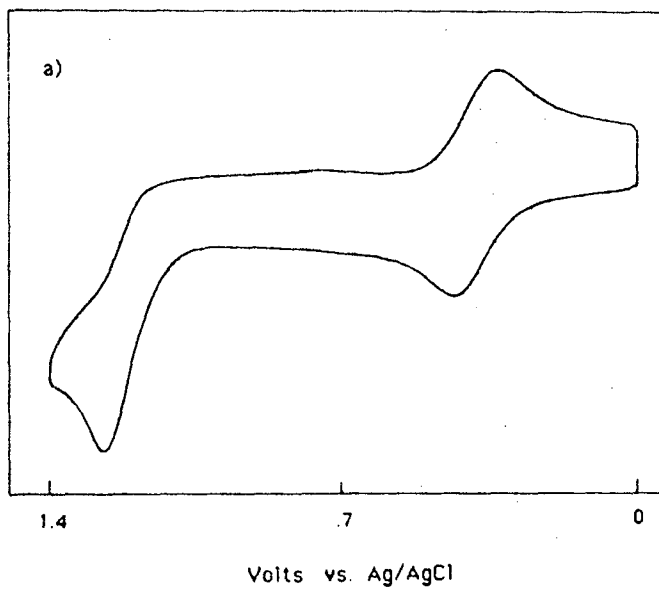
3. Methods

All melting points were taken in glass capillary tubes on a Melt-Temp laboratory Device and are reported uncorrected.

Elemental Analyses were performed by Galbraith Laboratories, Inc. in Knoxville, Tennessee.

Proton nuclear magnetic resonance spectra (^{1}H-NMR) were recorded using $CDCl_3$ as solvent. The 400 MHz spectra were recorded on a Bruker Model WH - 400 FT-NMR. The chemical shift data are reported in parts per million (on the δ scale) downfield from internal tetramethylsilane.

Carbon nuclear magnetic resonance spectra (^{13}C - NMR) were obtained using a Bruker Model WH - 400 FT-NMR and a Jeol Model FT - 100 with proton decoupling. The chemical shifts are in parts per million from internal tetramethylsilane.

High resolution mass spectra (MS) were recorded on a VG Analytical LTD 7035 mass spectrometer. Low resolution mass spectra (MS) were recorded on a Dupont 21 - 490B mass spectrometer at 75 eV unless otherwise noted.

IR spectra were recorded on a Perkin Elmer Model 467 infrared spectrophotometer.

Visible and UV were recorded on a Perkin Elmer Lambda-3 instrument interfaced to a Digital LSI - 11/03 computer.

Electrochemical data were recorded at 200 mV/s sweep rate by using a Princeton Applied Research Model 173 potentiostat in conjunction with a model 175 universal programmer. The reference electrode was a Ag/AgCl electrode (Bio-Rad). The electrolyte solutions were purged of oxygen by nitrogen bubbling. The $E_{1/2}$ values were obtained as the half-point potentials between the oxidative and reductive current-voltage peak

maxima and converted to values vs. NHE by adding 0.24V.

The working electrodes used were either Au, Pt, or glassy carbon electrodes supplied by Bio-Rad and were freshly polished before each use.

Static emission measurements were made in a Perkin-Elmer MPF - 44 A spectrofluorimeter.

Unless otherwise noted, materials were obtained from commercial suppliers and used without purification. In experiments requiring dry solvents, N,N-dimethylformamide (DMF) (J. T. Baker) was distilled from 4Å molecular sieves (Union Carbide) at reduced pressure and stored over 4Å molecular sieves. Benzene was dried by the addition of small pieces of sodium metal in the presence of benzophenone. The benzophenone turned from to blue when benzene was dry. The solvent was collected by vaccum distillation and kept under a dry nitrogen atmosphere.

Analytical and preparative thin layer chromatography (TLC) was carried out on silica gel plates purchased from Analtech, Inc. Column chromatography was carried out using Baker Reagent Grade Silica Gel (100 mesh).

References

1) M. -P. Pileni, A. M. Braun and M. Grätzel, Photochem. Photobiol., 31, 423 - 434 (1980).

2) P. -A. Brugger, P. P. Infelta, A. M. Braun, and M. Grätzel, J. Am. Chem. Soc., 103, 320 - 326 (1981).

3) F. M. Martens and J. W. Verhoeven, J. Phys. Chem., 85, 1773 - 1777 (1981).

4) A. Heller, Acc. Chem. Res., 14, 154 - 162, (1981).

5) H. Kuhn, J. Photochem., 10, 111 - 132 (1979).

6) D. Mobius, Acc. Chem. Res., 14, 63 - 68, (1981).

7) J. V. Beitz and J. R. Miller, Chem. Phys. Lett., 71, 4579 - 4595 (1979).

8) R. K. Huddleston and J. R. Miller, J. Phys. Chem., 86, 200 - 203 (1982).

9) R. K. Huddleston and J. R. Miller, J. Phys. Chem., 85, 2292 - 2298 (1982).

10) J. R. Miller, K. W. Hartman and S. Abrash, J. Am. Chem. Soc., 104, 4296 - 4298 (1982)

11) J. R. Miller, J. A. Peeples, M. J. Schmitt, and G. L. Closs, J. Am. Chem. Soc., 104, 6488 - 6493 (1982).

12) T. Guarr, M. McGuire, S. Strauch, and G. McLendon, J. Am. Chem. Soc., 105, 616 - 618 (1983).

13) S. Strauch, G. McLendon, M. McGuire, and T. Guarr, J. Phys. Chem., 87, 3579 - 3581 (1983).

14) B. H. Milosavljevic and J. K. Thomas, J. Phys. Chem., 87, 616 - 621 (1983).

15) H. Taube, Pure and Appl. Chem., 44, 25 - 42 (1975).

16) H. Fisher, G. M. Tom, H. Taube, J. Am. Chem. Soc., 98, 5512 - 5517 (1976).

17) C. A. Stein and H. Taube, J. Am. Chem. Soc., 100, 1635 - 1637 (1978).

18) C. A. Stein and H. Taube, J. Am. Chem. Soc., 103, 693 - 695 (1981).

19) C. A. Stein, N. A. Lewis, and G. Seitz , J. Am. Chem. Soc. , 104 , 2596 - 2599 (1982).

20) C. A. Stein, N. A. Lewis, G. Seitz and A. D. Baker, Inorg. Chem. , 22 , 1124-1128 (1983).

21) D. E. Richardson and H. Taube, J. Am. Chem. Soc. , 105 , 40-51 (1983).

22) H. M. McConnell, J. Chem. Phys. , 35 , 508-515 (1961).

23) K. A. Norton, L. G. Hulett, D. J. Halko, and J. K. Hurst, in "Tuneling in Biological Systems", Chance et al. (eds.) New York: Academic Press, pp. 237-241 (1979).

24) J. H. Borkent, A. W. J. De Jong, J. W. Verhoeven and T. J. Boer, Chem. Phys. Lett, 57 , 530 - 534 (1978).

25) J. H. Borkent, J. W. Verhoeven and T. J. De Boer, Chem. Phys. Lett, 42 , 50 - 53 (1976).

26) P. Pasman , J. W. Verhoeven and T. J. De Boer, Chem. Phys. Lett , 59 , 381 - 385 (1978).

27) P. Pasman , F. Rob and J. W. Verhoeven, J. Am. Chem. Soc. , 104 , 5127 - 5133 (1982).

28) L. T. Calcaterra, G. L. Closs and J. R. Miller, J. Am. Chem. Soc. , 105 , 670-671 (1983).

29) J. R. Miller, L. T. Calcaterra and G. L. Closs, J. Am. Chem. Soc. , 106 , 3047-3049 (1984).

30) J. L. Y. Kong and P. A. Loach , J. Heterocycl. Chem. , 17 , 737-744 (1980).

31) J. L. Y. Kong, K. G. Spears and P. A. Loach , Photochem. Photobiol. , 35 , 545-553 (1982).

32) I. Tabushi, N. Koga and M. Yonegita, Tetrahedron Lett. , 20 , 257-260 (1979).

33) T. F. Ho, A. R. MacIntosh and J. r. Bolton , Nature , 286 , 254-256 (1980).

34) A. Siemiarczuk, A. R. McIntosh, Te-Fu Ho, M. J. Stillman, K. J. Roach, A. C. Weedon, J. R. Bolton and J. S. Connolly, J. Am. Chem. Soc. , 105 , 7224-7230 (1983).

35) A. R. McIntosh, A. Siemiarczuk, J. R. Bolton, M. J. Stillman, Te-Fu Ho, A. C. Weedon, J. Am. Chem. Soc. , 105 , 7215-7223 (1983).

36) M. Migita, T. Okada, N. Mataga, S. Nishitani, N. Kurata, Y. Sakata, S. Misumi,

Chem. Phys. Lett., 84, 263-266 (1981).

37) S. Nishitani, N. Kurata, Y. Sakata, S. Misumi, M. Migita, T. Okada, N. Mataga, Tetrahedron Lett., 22, 2099-2102 (1981).

38) C. E. D. Chidsey and S. G. Boxer, Biophys. J., 33, 172 (1981).

39) N. Mataga, A. Karen, T. Okada, S. Nishitani, N. Kurata, Y. Sakata, and S. Misumi, J. Phys. Chem., 88, 5138 - 5141 (1984)

41) A. D. Joran, B. A. Leland, G. G. Geller, J. J. Hopfield, and P. B. Dervan, J. Am. Chem. Soc., 106, 6090 - 6092 (1984).

41) M. R. Wasielewski and M. P. Niemczyk, J. Am. Chem. Soc., 106, 5043 - 5045 (1984).

42) J. Dalton and L. R. Milgrom, J. Chem. Soc. Chem. Commun. 609 - 610 (1979).

43) M. A. Bergkamp, J. Dalton, and T. L. Netzel, J. Am. Chem. Soc., 104, 253 - 259 (1982).

44) S. G. Boxer, Biochim. et Biophys. Acta, 726, 265 - 292 (1983).

45) J. S. Lindsey, D. C. Mauzerall and H. Linschitz, J. Am. Chem. Soc., 105, 6528-6529 (1983).

46) P. Leighton and J. K. M. Sanders, J. Chem. Soc., Chem. Commun., 24 - 25 (1985).

47) T. A. Moore, D. Gust, P. Mathis, J-C. Mialocq, C. Chachaty, R. V. Bensasson, E. J. Land, D. Doizi, P. A. Liddell, W. R. Lehman, G. A. Nemeth and A. L. Moore, Nature, 307, 630 - 632 (1984).

48) S. Nishitani, N. Kurata, Y. Sakata, S. Misumi, A. Karen, T. Okada, and N. Mataga, J. Am. Chem. Soc., 105, 7771-7772 (1983).

49) D. Dolphin, J. Hiom, and J. B. Paine III, Heterocycles, 16, 417 - 447 (1981).

50) J. P. Collman, C. M. Elliott, T. R. halbert and B. S. Tovrog, Proc. Natl. Acad. Sci. U.S.A., 74, 18-22 (1977).

51) N. E. Kagan, D. Mauzerall, and R. B. Merrifield, J. Am. Chem. Soc., 99, 5484 - 5486 (1977).

52) J. P. Collman, P. Denisevich, Y. Konai, M. Marrocco, C. Koval, and F.C. Anson, J. Am. Chem. Soc., 102, 2699 - 2703 (1980).

53) I. Abdalmuhdi and C. K. Chang, J. Org. Chem., 50, 411 - 413 (1985).

54) R. R. Bucks and S. G. Boxer, J. Am. Chem. Soc., 104, 340 - 343 (1982).

55) C. K. Chang, M. S. Kuo, and C. B. Wang, J. Heterocycl. Chem., 14, 943 - 945 (1977).

56) T. L. Netzel, P. Krogen, C. K. Chang, I. Fujita, and J. Fajer, Chem. Phys. Lett., 67, 223-228 (1979).

57) I. Fujita, J. Fajer, C. K. Chang, C. B. Wang, M. A. Berkamp, and T. L. Netzel, J. Phys. Chem., 86, 3754 - 3759 (1982).

58) T. L. Netzel, M. A. Berkamp, C. K. Chang, J. Am. Chem. Soc., 104, 1952 - 1957 (1982).

59) R. R. Bucks, T. L. Netzel, I. Fujita, and S. G. Boxer, J. Phys. Chem., 86, 1947-1955 (1982).

60) I. M. Gund, Y. Z. Williams, Jr., E. Osawa, and P. v. R. Schleyer, Tetrahedron Letters, 44, 3877 - 3880 (1970).

61) T. M. Gund, E. Osawa, Y. Z. Williams, Jr., and P. v. R. Schleyer, J. Org. Chem., 39, 2979 - 2987 (1974).

62) T. M. Gund, M. Nomura, Y. Z. Williams, Jr., and P. v. R. Schleyer, Tetrahedron Letters, 56, 4875 - 4878 (1970).

63) T. M. Gund and P. v. R. Schleyer, Tetrahedron Letters, 19, 1583 - 1586 (1971).

64) T. M. Gund, P. v. R. Schleyer, G. D. Unruh, and G. J. Gleicher, J. Org. Chem., 39, 2995 - 3003 (1974).

65) N. Hush and J. R. Miller, Personal comunication.

66) H. Koch and W. Haaf, Angew. Chem., 72, 628 (1960).

67) H. Koch and W. Haaf, Org. Synthesis, 44, 1 - 3 (1964).

68) G. H. Barnett, M. F. Hudson and K. M. Smith, Tetrahedron Letters, 2887-(1973), and references therein.

69) R. G. Little, J. A. Anton, P. A. Loach and J. A. Ibers, Heterocyclic Chem., 12, 343 - 349 (1975).

70) J. A. Anton and P. A. Loach, Heterocyclic Chem., 12, 573 -576, (1975).

71) F. E. Mayer, D. L. Cullen in "The Porphyrins"; D. Dolphin, Ed.; Academic Press New York, (1979); Vol. 3, p 513

72) S. S. Eaton, G. R. Eaton, J. Am. Chem. Soc., 99, 6594 - 6599 (1977), and references therein.

73) J. C. Curtis, B. P. Sullivan, and T. J. Meyer, Inorg. Chem., 22, 224-236 (1983) and references therein.

74) S. S. Isied and H. Taube, Inorg. Chem., 13, 1545 - 1551 (1974).

75) S. S. Isied and H. Taube, Inorg. Chem., 15, 3070 - (1976).

76) J. E. Falk, in "Porphyrins and Metalloporphyrins"; Elsevier: New York, (1964); pp 72 - 80, 89 - 93.

77) F. A. Walker, Y. L. Balke, and G. A. McDermott, Inorg. Chem., 21, 3342-3348 (1982), and references therein

78) T. Gund, Ph. D. Dissertation, Princenton (1973).

79) L. H. Vogt, J. S. Katz, S. E. Wiberly, Inorg. Chem., 4, 1156 - (1965).

CHAPTER   III

Photoinduced Electron Transfer in Bifunctional

Porphyrin - Ru(III) Ammine Complex

INTRODUCTION

In the last decade, much theoretical and experimental progress has been made in understanding the factors which govern the rates of electron transfer reactions. Recently much attention in the field of electron transfer studies has been devoted to important and poorly understood parameters, such as the distance and orientation between the donor and acceptor, and the driving force in nonadiabatic systems. The distance dependence of the rate of electron transfer between redox partners is predicted by recent theory [1-4] to be :

$$k_{ET} = C \, |H_{ab}|^2 \, [FC] \qquad (1)$$

where
$$|H_{ab}| = Y_0 \exp(-\alpha R) \qquad (2)$$

α = is a factor which is proportional to the energy difference between the electron donor and the medium

R is the distance between localized electronic sites,

C and Y_0 are constants,

and [FC] represents the Franck-Condon term.

It is clear from equation (2) that the rate of electron transfer has a strong exponential dependence on distance (i.e. orbital overlap) which is contained in the electronic coupling matrix element, $|H_{ab}|$.

The equation also predicts the dependence of rate on ΔE, E_r, and temperature through the Franck-Condon weighted density of states factor, [FC]. In the high-temperature, strong coupling limit, the model reduces to the classical Marcus equation[2]:

$$K_{ET} = A \exp \left[\frac{-(\Delta E - E_r)^2}{4 E_r KT} \right] \tag{3}$$

where

$$A = 2\pi |H_{ab}|^2 / \hbar^2 \omega \tag{4}$$

and

E_r is the total reorganization energy

The classical Marcus model has been applied successfully to explain electron transfer in adiabatic systems. However, relatively little is known about either the distance or driving force dependence of nonadiabatic systems. Nonadiabatic reactions are ubiquitous in biological systems since the reactants are separated by large distances[2-6].

Several experiments which were designed to probe the distance dependence as well as the driving force dependence of electron transfer are discussed in detail in chapter II. The most promising systems are molecular adducts which contain both reactants and products which are covalently attached by a rigid molecular spacer. Relatively few of these bifunctional molecules have so far been prepared, but these systems have provided very useful information, since it is possible to measure the effects of rate on ΔE[7], reactant separation[8] and orientation[9] without the complications inherent in diffusional systems. For example, Miller et al.[7] have reported the first experimental evidence of the controversial Marcus "inverted region".

Furthermore, new questions arise from such systems. For example, Closs and Miller [10] have studied electron transfer in bifunctional steroids. They found $k_{et} >$ $10^6 s^{-1}$, at ≈ 15 Å donor-acceptor separation and $\Delta E \approx 0.1$ V, whereas Gray et al [11] reported $k_{et} \approx 20 s^{-1}$ in Ru(III) substituted cytochrome c at similar driving force and donor-acceptor separation. It seems that the nature of the reagents, and /or the intervening material can dramatically alter the rates of electron transfer reactions. In addition the angular alignment between two aromatic redox partners may play a significant role in optimizing the rate of electron transfer.

The use of porphyrins in studies of photoinduced electron transfer reactions has been growing in the last few years. One advantage of using porphyrins is that the charge can be created by photoexcitation of the porphyrin. Otherwise, if the system lacks the presence of the luminescent chromophores, the charge must be created by the use of a third species, or by pulse radiolysis, which brings complications that are inherent to each technique adopted.

In most of the photoinduced electron transfer studies, the porphyrins are covalently linked to quinones by a flexible linkage which allows both the distance and orientation between the donor and acceptor to vary widely [12 - 21]. Recently a new class of porphyrin-quinone adducts where the donor and acceptor are linked at a fixed distance have been reported [6 - 9, 22]. For example, Wasieleswski and Namczyk [8] reported a very efficient quenching of the singlet excited state in a Porphyrin-quinone system, linked by a rigid spacer, but the presence of a hydrocarbon spacer could play a significant role as a possible transmission line for the electron transfer.

More information can arise from studies of new classes of molecular adducts by

varying the nature of the spacer and of the reagents. To this end we prepared a new class of bifunctional porphyrin-Ru(III) ammine complexes of the general structure:
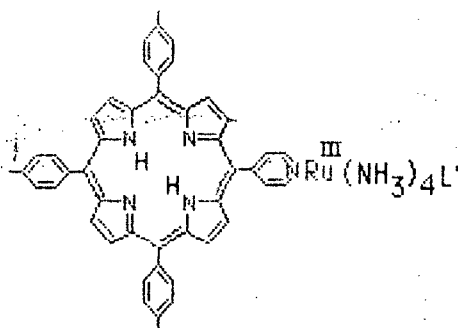
I : L' = NH3
II : L' = Py
III : L' = (3-Cl-Py)

In the above structure, the pyridine ligand is held essentially perpendicular to the porphyrinic ring so π- orbital overlap between both reactants is minimized. X - ray diffraction results on tetra-meso-arylporphyrins indicate that the dihedral angle between the phenyl rings and the porphyrin is 61 - 63 º. [23 - 24] In addition, the reaction driving force, ΔE can be systematically varied by appropriate replacement of the trans ligand in the sixth coordination position of the ruthenium complex.

The first goal of this work is the study of photoinduced electron transfer in these complexes as a function of the driving force. The rate is expected to increase with increasing driving force as predicted by the theoretical models for electron transfer. The P-Ru(III) system can provide all necessary information to test this prediction.

Secondly, it is expected that the relative orientation of the pyridine ligand might play a significant role in optimizing the rate of electron transfer. The extent to which angular orientation of the reactants effects the rate of the electron transfer, and thus

the adiabaticity of the system, can be adressed by this system. The intramolecular rates observed in the bifunctional porphyrin where the porphyrin-pyridine orientation is fixed, are compared with the intermolecular rates observed in the diffusional encounter reaction involving monosubstituted porphyrin and unbound $Ru(III)(NH_3)_5 Py$ complex, since in the diffusional case, all pyridine-porphyrin orientations are possible. Therefore, measurements involving the diffusional photoinduced electron transfer between monosubstituted porphyrin and varying concentrations of the unbound $Ru(III)(NH_3)_5 Py$ complex will be performed.

Finally, it will be useful also to compare the rates observed in P-Ru(III) system with the rates observed in a homologous system described recently by Netzel et al.[22] In the latter system a quinone is attached to the meso position of the porphyrin and the relative orientation between both rings is also expected to be "nearly" perpendicular.

1. Materials and Methods

Material

The solvents were all reagent grade. In experiments requiring dry solvents, N,N-Dimethylformamide (DMF) was distilled from 4 Å molecular sieves (Union Carbide) at reduced pressure. Methylene Chloride were purchased from J. T. Baker as Spectrophotometric Grade Solvent . Solvents were allowed to stand over 4 Å molecular sieves.

Methods

Static emission measurements were made in a Perkin-Elmer MPF - 44 A spectrofluorimeter. Samples of free ligand porphyrin and modified porphyrin were adjusted to the same concentration, using a Perkin Elmer Lambda-3 instrument. Excitation wavelengths correspond to the Soret peaks (λ = 480nm), and emission was monitored at the maximum of the emission band.

Laser flash photolysis studies were carried out by using a Quanta-Ray DCR-2 Nd:YAG . The second harmonic (λ = 532 nm), ca, 250 mJ per pulse and a flash duration of 8 ns; was used as the excitation source. A monitoring tungsten lamp was used. A shutter which was controlled by the computer and synchronized with the laser, minimized the time that the sample was exposed to light. The signal collected from a 1P28 photomultiplier was amplified by a FET probe amplifier and input into a waveform Biomation 6500 transient digitizer. The system was interfaced to a Digital LSI - 11/03 computer which controlled the firing of the laser.

The kinetics were monitored by observing the return of the porphyrin signal (bleaching of the Soret) or by observing the transient triplet-triplet absorption in the 450 nm region, where the triplet-triplet absorption band characteristic of free base porphyrins predominates[25].

The values of the triplet excited state lifetime decay were obtained from the Single Exponential Linear Least-Squares Fit program.[26] It is assumed here that the molecular luminescence obeys a single exponential decay leading to an expression of the form:

$$I(t) = I_0 \exp(-t / \tau) \tag{5}$$

where I is the intensity of transmited light for a particular time t of the $T_1 - T_2$ absorbance decay curve, I_0 is the initial intensity and τ is the excited state lifetime decay. Dates were converted to absorbance (assuming zero baseline) and a fit was obtained from plot of ln A vs time yielding a straight line (assuming a single exponential decay).The slope yields the lifetime and the fit yields the calculated fit data curve.

1 cm quartz cells were used and samples were degassed by the freeze-pump-thaw method. Measurements were also made in a Ar-purged solution and both methods proved to be efficient in eliminating oxygen from the solution.

The porphyrins under study follow Beer's law in DMF over a concentration range of 10^{-5} to 10^{-6} M. The fact that the Beer's law holds over this concentration range indicates that oligomer formation and stacking is negligible.

2. Results and Discussion

The rate of photoinduced electron transfer in the system under study is experimentally determined as the difference between the rate of triplet decay for the free ligand porphyrin and the modified one, ie;

$$k_{ET} \quad 1/\tau - 1/\tau_o \tag{6}$$

where τ_o represents the triplet decay lifetime of the unmodified porphyrin (free ligand) and τ is the triplet decay life time of the modified porphyrin. Thus the rate of excited state decay of the modified porphyrin is expected to be much larger than that for the free ligand porphyrin, since the presence of an electron quencher in the meso pyridine opens a new (and not surprisingly) efficient competing decay channel.

The population of the porphyrin triplet excited state is facilitated by the relatively small S - T splitting, high intersystem crossing yield and long triplet lifetime[27] of the porphyrin chromophore. The determination of the triplet state decay, obtained by monitoring the $T_1 \longrightarrow T_2$ absorption spectra. Shown in Figure 1. is a state diagram showing the pathway leading to $T_1 - T_2$ absorption. Absorption in $\underline{a}$ is followed b; intersystem crossing $\underline{b}$, to populate T_1. It is then capable of absorbing photons and undergoing $T_1 \longrightarrow T_2$ transitions. The electron transfer pathway to the acceptor is shown as well as the spontaneous triplet decay. The kinetic information was obtained from transient absorption measurements of the bifunctional porphyrin dissolved in DMF at room temperature.

The triplet excited state decay of free ligand porphyrin, 5 - (4 - Pyridyl) - 10, 15,

Figure 1. State Diagram Showing the Electron Pathway Leading to the Reduction
of Acceptor

Donor   Acceptor
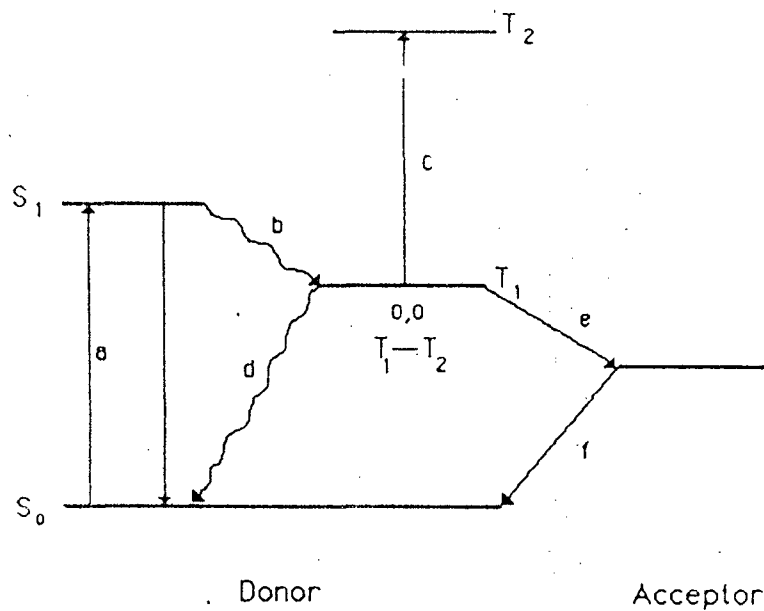
20-tritolyl-porphyrin was observed by monitoring the T-T absorbance at 450 nm. The resulting excited state decay is shown in Figure 2. The decay curve shows a single exponential decay over the first 65% of the total reaction. Lower correlations were obtained if the entire range of the decay curve were measured. The result suggest several possibilities: First, gross errors could have been made during the baseline subtraction since the baseline is not flat in the time base used (time base of 500 ns per channel was used) Second, more than one decay may occur if the free ligand porphyrin presents more than one conformation in solution. Another possibility is that the pyridine may be protonated, but this possibility is unlikely in DMF. The presence of a second excited decay was observed by another research group, using homologous systems[28].

The triplet excited decay of the modified porphyrin is shown in Figure 3. Our results show that the incorporation of a neighboring Ru(III) center in the meso pyridyl, modifies the reactivity of the porphyrin moiety. The rate of the triplet excited state decay is reduced from $6.5 \times 10^3 s^{-1}$ for free porphyrin ligand to $4 \times 10^4 s^{-1}$ for the meso-tritolyl [N - (pentaammineruthenium)(III) pyridyl]porphyrin (I).

The observed quenching of the triplet excited state was tentatively assigned to a photoinduced electron transfer process from the porphyrin excited state to the ruthenium. In order to test this assignement we chose to vary the exothermicity of the system since for electron transfer the rate depends on the exothermicity for reaction. To acheive this goal in the Porphyrin - Ru system, the driving force of the system was changed by varying the redox potential of the ruthenium. Thus, the redox potential of the Ru(III) was altered by replacing the amine "trans" ligand on ruthenium with ligands that are π acceptors. The Ru (III, II) formal potentials acquire more positive values as the π - accepting capability of the sixth ligand increases. The amino ligand on the trans

Figure 2. Decay of T-T absorption of 5-(4-pyridyl)-10,15,20-tritolyl-porphyrin in DMF observed at 450nm. Average of 50 laser shots. Continuous line shows the theoretical correlation (C = 99%) for 65% of the reaction.

INTENSITY

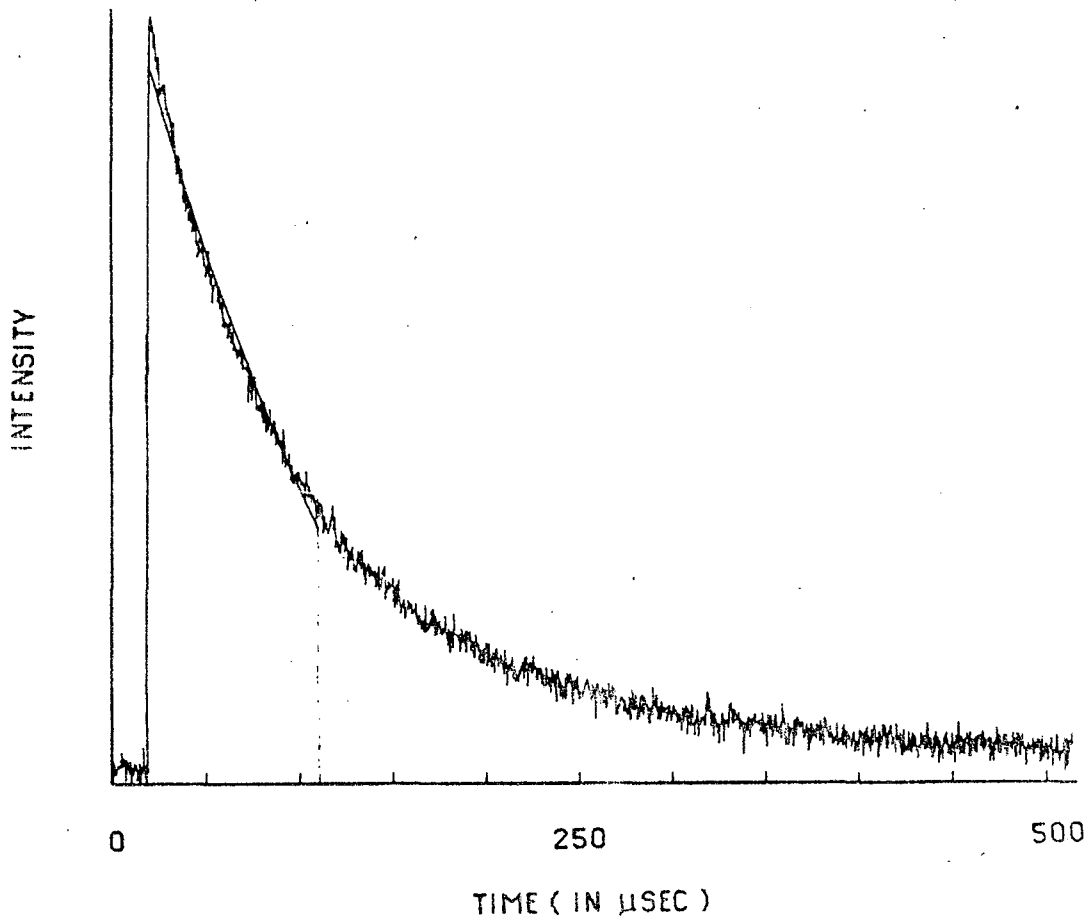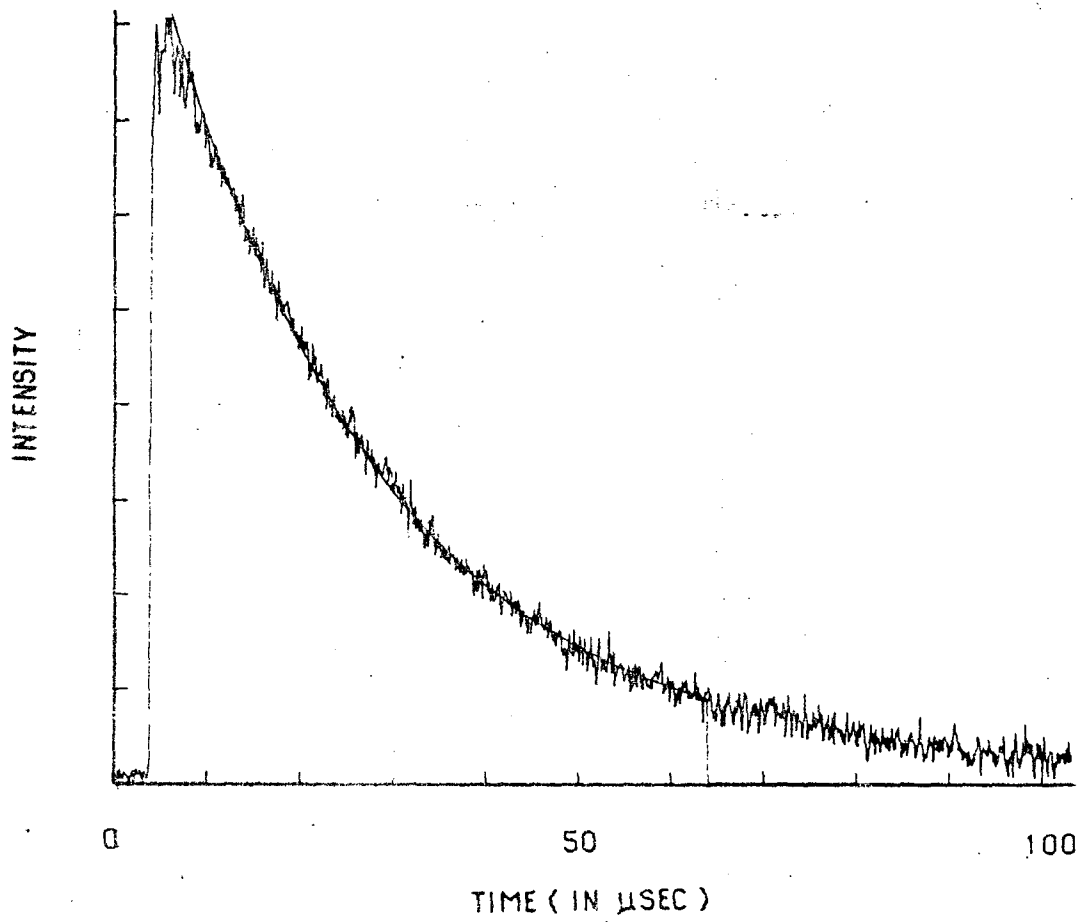TIME (IN μSEC)

0   250   500

Figure 3. Decay of T-T absorption of $H_2TTP(p-CH_3)_3(4-Py)Ru^{III}(NH_3)_5$ in DMF observed at 450nm. Average of 60 laser shots. Continuous line shows the theoretical correlation ($C > 99\%$) for 90 % of the reaction.

INTENSITY

TIME (IN μSEC)

position of the ruthenium was replaced by pyridine and 3-Cl-Py. The driving force, ΔE, for each molecule is the resulting sum of the one - electron oxidation potential and the one-electron reduction potential for each molecular adduct. For the Porphyrin- Ru system, ΔE is estimated using

$$\Delta E = E(P / P^+) + E(Ru^{3+}/Ru^{2+}) \tag{7}$$

The difference between this energy and the energy of the lowest triplet excited state of the porphyrin, yields then an estimate of the exothermicity of the photoinduced electron transfer reaction. We assume that the entropy change of the $S_0 - T_1$ process is negligible. Thus the exothermicity is estimated using

$$\Delta U = \Delta G - E_{0-0}(P - {}^3P^*) \tag{8}$$

For exar , based on the cyclic voltammogram datas shown in table I, we estimated, a value of $+ .07\,eV$ for the free energy of the ground state of P-Ru system. Combined with a value $E_{0-0}(P - {}^3P^*) = 1.44\,eV$, $\Delta U = -0.37\,eV$ was estimated for the excited triplet state. It is clear that is easier to achieve electron removal from an excited state than from the ground state. Another important point to be noted is that the exothermicity of the P-Ru(III) system can also be altered by following the transfer from the singlet excited states or by incorporating a metal into the porphyrin.

The resulting values for the photoinduced electron transfer as a function of the exothermicity are displayed in table II. The triplet excited state decays for compounds II and III is shown in Figures 4 and 5.

The rate of the excited state decay increases (Figures 4 and 5) following the order:

$${}^3k_{free\ ligand} < {}^3k_{NH3} < k_{pyr} < k_{3-Cl-Py}$$

Table II: $E_{1/2}$ Values vs the NHE in DMF (V)

Compd		$E_{1/2}$ ($Ru^{III/II}$)	$E_{1/2}$ $p^{+/0}$
[P Ru(NH$_3$)$_5$](PF$_6$)$_3$[a]		0.40	1.47
[tr-P Ru(NH$_3$)$_4$Py](PF$_6$)$_3$		0.58	1.43
[tr-PRu(NH$_3$)$_4$(3-Cl-Py)](PF$_6$)$_3$		0.66	1.44

[a] P = Meso-H$_2$TPP(pCH$_3$)$_3$(4PY)
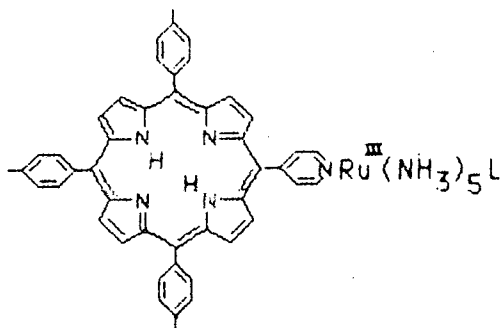
Table II Rate of Electron transfer and driving force P-Ru(III)
Homologues

Compd	ΔE^b (V)	k_{ET}^c (s^{-1})
[P Ru(NH$_3$)$_5$](PF$_6$)$_3$[a]	0.38	4.0×10^4
[tr-P Ru(NH$_3$)$_4$Py](PF$_6$)$_3$	0.55	1.2×10^5
[tr-PRu(NH$_3$)$_4$(3-Cl-Py)](PF$_6$)$_3$	0.63	5.0×10^5

a - P = Meso-H$_2$TPP(pCH$_3$)$_3$(4PY)

b - Measured using $\Delta E = E_{o-o}(P - {}^3P^*) + E(Ru^{3+}/Ru^{2+}) - E(P^+/P^o)$

$E_{o-o}(P - {}^3P^*)$ = has taken as 1.44 eV [25]

c - Measured using Eq. 6

Figure 4. Decay of T–T absorption of $H_2TTP(p-CH_3)_3(4-Py)Ru^{III}(NH_3)_4Py$ in DMF observed at 450nm. Average of 60 laser shots. Continuous line shows the theoretical correlation (C > 99%) for 90 % of the reaction.

INTENSITY

TIME (IN μSEC)

Figure 5. Decay of T–T absorption of $H_2TTP(p-CH_3)_3(4-Py)Ru^{III}(NH_3)_4(3-Cl-Py)$

in DMF observed at 450nm. Average of 150 laser shots. Continuous line

shows the theoretical correlation (C > 99%) for 90 % of the reaction.

INTENSITY

TIME (IN μSEC)

0   5   10

The observed results were interpreted in terms of the classical Marcus theory [29-31]. As already mentioned, this theory assumed that all electron transfer reactions occur on an adiabatic potential surface, which is formed by an avoided crossing of the reactants and products caused by a strong electronic interaction.
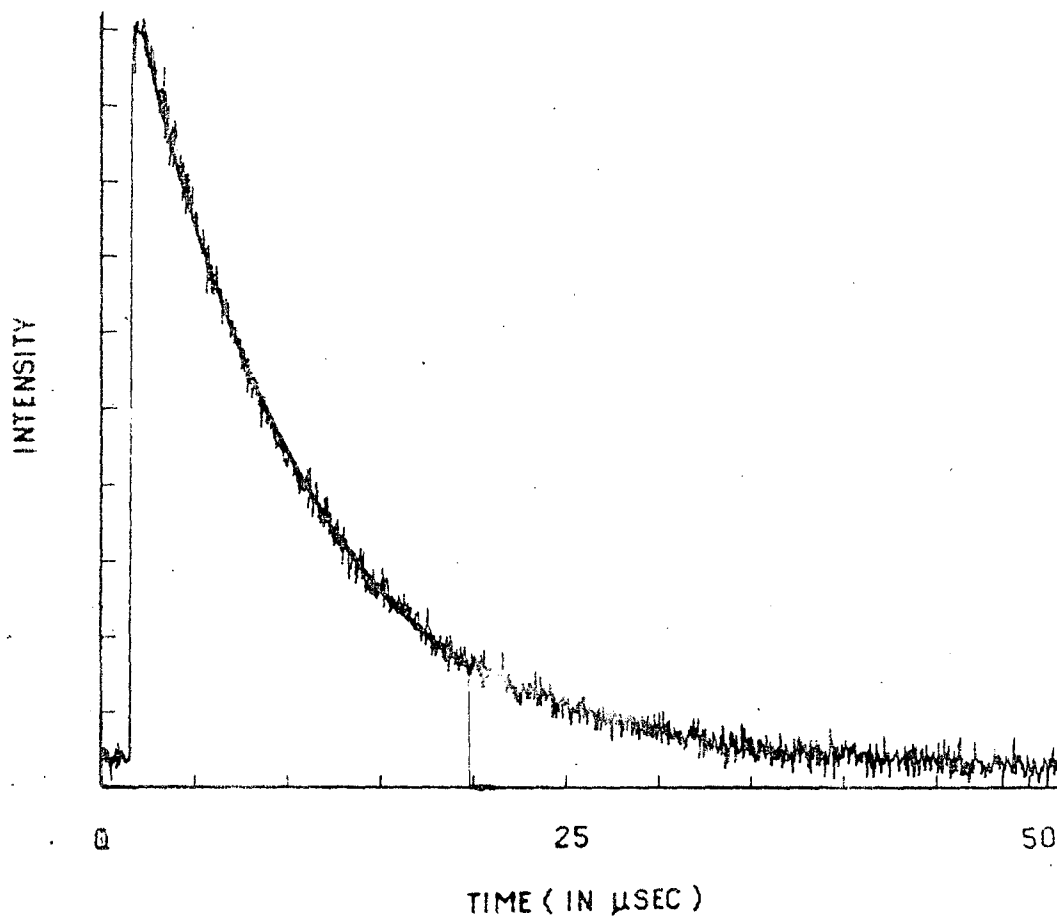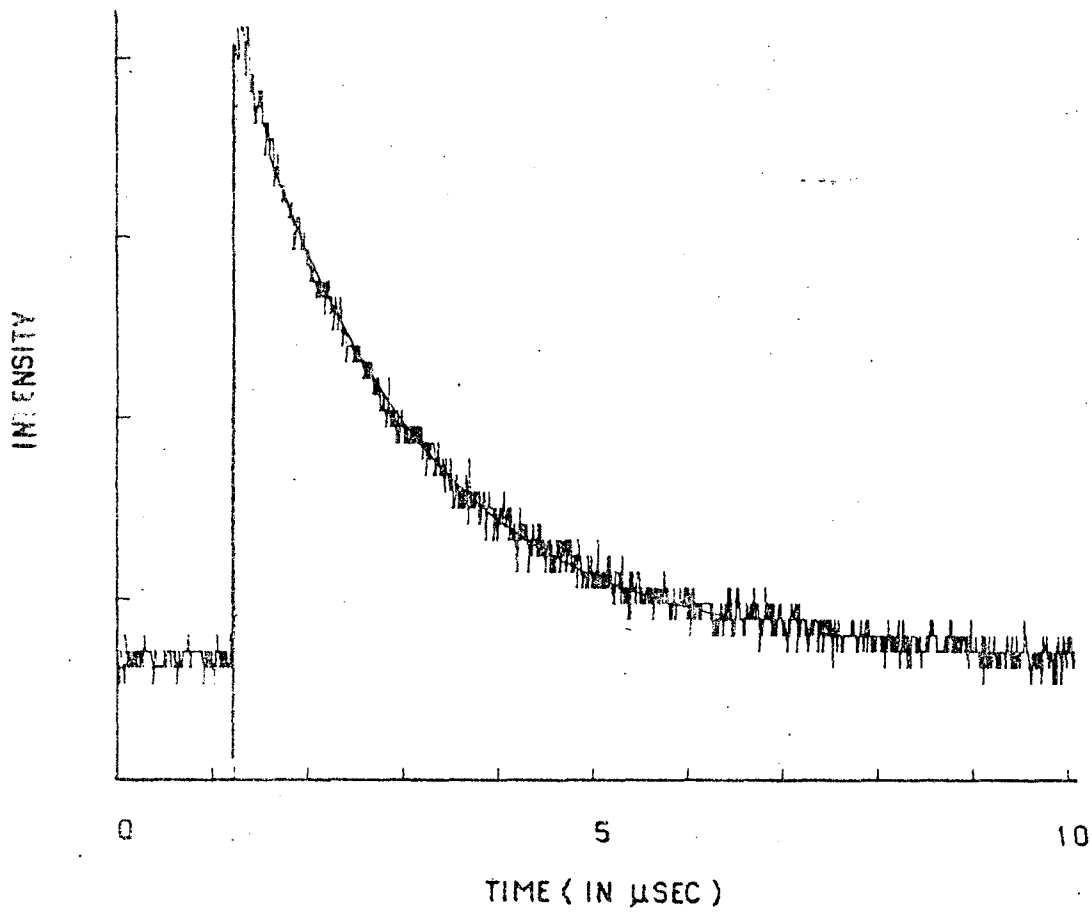
The rate constant for a photoinduced electron transfer may be written as

$$K_{ET} = A \exp \left[\frac{-(\Delta U + E_r)^2}{4 E_r KT} \right]$$

(9)

where A is a preexponential factor, which in the classical theory is simply a collision frequency [29-31], E_r is the total reorganization energy. As already mentioned E_r represents the sum of the internal (λ_i) and external (λ_s) reorganization energies. λ_i is due to the bond length and bond angle deformations, and λ_s is due to the solvent repolarization energy.

This theory predicts that the rate of electron transfer increases with increasing exothermicity. Indeed, this prediction is confirmed for the system under study, as is clearly indicated by the plot of lnk vs. ΔU (Figure 6). The best agreement between theory and experiment is obtained if one uses a value of 0.8 V for E_r. This fact is strongly suggestive that electron transfer is the dominant reaction pathway, but energy transfer pathways are not automatically precluded. Three other mechanisms could produce the quenching of triplet excited state of porphyrin: (1) energy transfer from the porphyrin excited states to pentaammine Ruthenium states and back to ground porphyrin states; (2) "Heavy-atom" quenching which catalyzes the fast radiationless decay routes. (3) Exchange quenching, (4) or magnetic dipole quenching.

Figure 6. Plot of log of the photoinduced electron transfer vs. the free energy change of the electron transfer reaction. The continuous line was calculated by using the Marcus free energy relationship (eq. 9) $E_r = 0.8\,eV$.
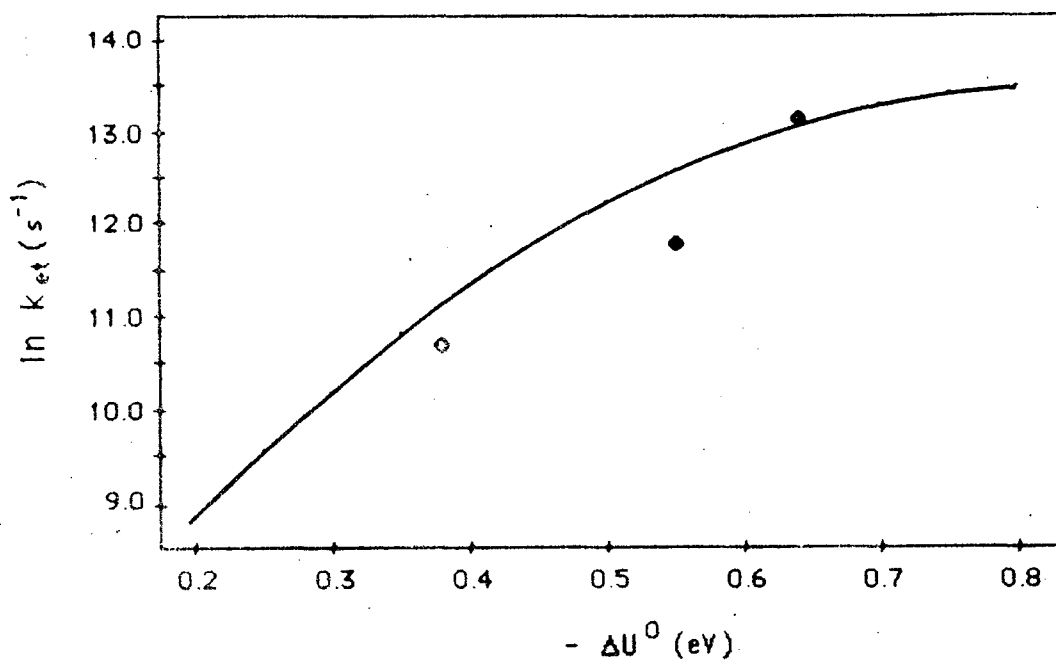
The first possibility is excluded since energy transfer from the lowest porphyrin triplet excited state (1.44 ev) [32] to the lowest pentaamin ruthenium states ($\approx$ 3 ev) [33] is too endothermic to be considered important.

If the observed quenching of the lowest porphyrin triplet excited state is due to a "heavy-atom" quenching, the same change in the reactivity of the porphyrin should be observed when the Ru (III) is reduced to Ru (II). Kinetics results of P-Ru(II) shows the same triplet excited decay that was observed in the free ligand porphyrin, thus eliminating the possibility of the deactivation via the second mechanism.

The third and fourth possibilities seem to be remote since, the ruthenium III species is located considerably far from the center of the ring, where such effects could be effective. The synthesis of a non reducible Ru (III) species is suggested to elucidate this point.

To provide more direct evidence of redox product formation a kinetic competition experiment was performed. The experiment consisted of irradiating (III) in DMF. It is known that porphyrins can mediate the photooxidation of a variety of organic substrate [27] and photoxidation of DMF by porphyrins has been observed [34]. The porphyrin triplet excited state does not react directly with DMF ($\tau_{DMF} = \tau_{CH3CN}$). The resulting kinetic competition experiment shows that when (III) is irradiated in DMF, Ru (III) is reduced to Ru (II), but no such reaction occurs in CH_3CN. Figure 7. shows the visible spectra of P-Ru(III) systems before and after photolysis. The spectra obtained after photolysis is characteristic of the P-Ru(II) system. This fact provides evidence for a clear case of intramolecular electron transfer, followed by solvent oxidation by the porphyrin cation radical.

Thus, the experiments reported here provid evidence that the triplet excited state of the porphyrin moiety sensitizes the electron transfer to the Ruthenium complex. From these studies it is clear that in the normal free energy region, the quadratic dependence of ln k on ΔU predicted by the Marcus theory is basically correct.

We felt that it would be of interest to examine the return of an electron to porphyrin by monitoring the reappearance of the soret band after bleaching (bleaching is caused by a loss of an electron from the ground state). It was observed that the rate of back electron transfer is faster than the forward electron transfer rate. Therefore the rate of forward electron transfer is rate determining in the repopulation of the ground state porphyrin. Such a result is expected, since for $\lambda \approx 0.8$ V, k_{ET} back $\geq k_{ET}$ forward.

It is interesting to compare the result observed from compound (III), where the rate of 5.0×10^5 s^{-1} was observed at $\Delta G \approx -0.64$ V with that found in structurally homologous porphyrin quinone system (IV) (10^{11} s^{-1}) at $\Delta G \approx -0.02$ V [22]. Two points

IV
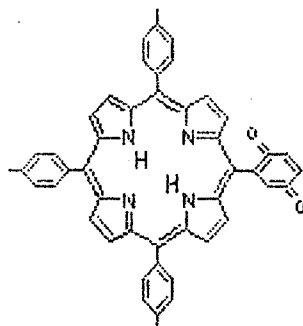
must be emphazised here:

1) In both systems the distance and orientation between donor and acceptor appear to be similar.

2) The Franck Condon factors are optimized in the porphyrin-Ru(III) system, but not in the porphyrin quinone.

The obvious question that arises is; How can such dramatic diference of six orders of magnitude in rate be explained ?

The synthesis of the system under study was based on the simple fact that the orientation between the pyridine and porphyrinic ring ensures weak electronic coupling, and thus reduces the adiabaticity of the electron transfer.

This strategy appears to work in this system and the low observed rate could reflect the orientation between both reactants even though the porphyrin and ruthenium complex are in intimate contact. ($\leq$ Van der Waals contact)

It is interesting to note that data of Wasielewski et al [9] suggest a rate $> 10^{10} s^{-1}$, at $\Delta G \approx -0.70$ in a molecule where the the π electronic system of the porphyrin maintains a 6 Å edge-to-edge separation with that of the quinone in a parallel fashion. It seems that the rate here is optimized by the proper orientation of donor and acceptor.

Our results on the electron transfer reactions can be utilized in conjunction with the classical and/or quantum mechanical models to obtain an estimate of the distance traveled by the electron. DeVault [35] derived an equation for the probability of an electron transition passing from the reactant potential surface R to the product potential surface P at a any given energy. In his derivation the nuclear motion was treated classically but the probability P_{RP} of an electronic transition from R to P was derived

by the Landau and Zener equation. The resulting equation is a combination of Equation 3 and:

$$A = 2\pi/\hbar \, |H_{ab}|^2 \, (4 \pi E_r K_B T)^{-1/2} \qquad (11)$$

Thus structural information about the separation of the electron donor and acceptor might be obtained through the prefactor A. Calculations based on this formula give $|H_{ab}|$= 3.2×10^{-2} cm^{-1} which is surprisingly nonadiabatic for a system in which donor and acceptor are in close contact. Equation 2 was used to calculate the distance R given the constant $\alpha = 1/a$, where the parameter a is expressed in the same units of R and was estimated from pulse radiolysis studies suggesting a ≈ 0.75 Å [36]. We expect that the relative angular orientation between donor and acceptor could cause a large effect on $|H_{ab}|$. In this calculation such an effect was not considered, and the adopted value of 0.75 Å for the constant "a" reflects an average of angular distributions. This analysis of our experimental findings allows us to estimate the distance travelled by the electron as being about 11 Å. It appears that the electron travels from the edge of the prophyrin ring to the center of ruthenium atom, probably via a through space pathway. This distance was calculated by CPK models as being about (≈ 7 Å), while the center-to-center distance is ca. 10 Å. The edge is defined as that position one space parameter away from the maximum in π-electron density.[37]

To our knowledge this is the first case of nonadiabatic electron transfer reaction where the redox centers are at a close contact. The demonstration that the rates of electron transfer are nonadiabatic even at the Van der Waals distance adds support to recent suggestions that the degree of adiabaticity in many diffusional electron transfer

reactions can be low.[38]

The quenching of $H_2TTP(p-CH_3)_3(4-Py)$ in a DMF solution containing various concentrations of unbound $Ru^{III}(NH_3)_5 Py$ [(1- 30) X 10^{-4} M] show that (Figure 8) the rate of electron transfer increases linearly with ruthenium complex concentration at low values and then more rapidly, suggestive a very efficient static quenching mechanism. No rate saturation was observed at the highest concentration of Ruthenium complex, suggestive of static quenching. Such static quenching is well established for quenching of porphyrins by other aromatics acceptors.[39]

Surprisingly, the intermolecular rate of quenching of $H_2TTP(p-CH_3)_3(4-Py)$ exceeds the corresponding intramolecular quenching rate in compound (I) even at low concentration of the quencher. It is interesting to note that in (I), the "quencher" portion of the molecule is obviously already in "collisional" contact with the porphyrin. The observed rates in bimolecular reaction are faster than the corresponding unimolecular reactions. The maximum bimolecular rate is set by the solubility of $Ru(III)(NH_3)_5PY$ and it is 100 times faster than the rate observed in (I).

Orientational averaging is expected for a collisional electron transfer reaction, and a proper orientation could lead to higher adiabaticity than that achieved for the dimetallic porphyrin where the geometric constraint tends to minimize the rate of electron transfer.

The reactants in the bimolecular study allow the formation of two different geometries which might optimize the rates of diffusional electron transfer:

1) Attack by the "ammine" face, reducing the distance between the porphyrin and ruthenium.

2) Coplanar attack of pyridine in the porphyrin ring (most probably over the pyrrole ring) resulting in a stacking geometry between the porphyrin and pyridine.

Calculations by Marcus and Siders[40] predict that the relative orientation between two π-system plays an important role in optimizing the rate of electron transfer. For example, the rate is optimized in a stacking geometry, and minimized in a perpendicular orientation. This prediction provides support for the latter explanation.

Summary

Summarizing our results, we note that the photoinduced electron transfer in a P-Ru(III) system depends on the driving force of the system and the rate increases following the order: $k_{free\ ligand} < k_{NH3} < k_{Py} < K_{(3-Cl-P)}$. This results are interpreted in terms of the classical Marcus theory, which predicts a quadratic dependence of lnk on ΔU. From these data an estimate of the reorganization energy is obtained: $E_r = 0.8\ eV$. Theoretical analysis of our results allows us to estimate the degree of adiabaticity as being $|H_{ab}| = 3.2 \times 10^{-2}\ cm^{-1}$ which is surprisingly nonadiabatic for a system in which donor and acceptor are in close contact.

To our understanding, this is the first case of a nonadiabatic electron transfer reaction in which donor and acceptor are in a Van der Waals contact. Such findings may have important biological implications. At least two explanation are possible:

1) Perhaps the relative orientation between the pyridine and porphyrin ring plays an important role in optimizing the rate. The meso pyridine in the bifunctional porphyrin is constrained essentially perpendicular to the porphyrin plane, due to steric interference caused by the β-pyrrole and o-pyridine protons. Thus π-π overlap is minimized. In the absence of strong aromatic coupling, it appears that the transfer occurs directly to the ruthenium atom, probably via a through space pathway. By contrast, in analogous prophyrin quinone systems the through space path is much shorter, consistent with the faster rates observed in such systems. This explanation is consistent with calculations of Marcus and Siders.[40] However, at a 60° relative angle one would expect relatively large overlap.

2) In the reactive electronic state, little or no density resides at the meso carbon,

so that a through bond pathway is effectively prevented. Some support for this notion is available from the claculation of Gouterman et al.[41]

We concluded that nonadiabaticity can occur, even at the Van der Waal distances between reactants, if the interaction geometry is not optimized. The distance traveled by the electron was estimated to be 11 Å, which is consistent which a center-to-center distance between both redox partners.

The observed rates in bimolecular reaction, between unsubstituted porphyrin and the Ru(III)(NH$_3$)$_5$Py are 100 times faster than found in unimolecular Porphyrin-Ru(III) systems. This fact might be understood in similar geometric terms. In the bimolecular reaction, π-π overlap of the porphyrin and pyridine may occur, leading to an increase in effective rate.

REFERENCES

1) G. Gamow, _Z. Phys._ , _51_ , 204 - 212 (1928).

2) J. J. Hopfield, _Proc. Natl. Acad. Sce. U.S.A._ , _71_ , 3640 - 344 (1974).

3) J. Jortner, _J. Chem. Phys._ , _64_ , 4860-4867 (1976).

4) A. M. Kuznetzov, N. C. Søndergård, and J. Ultrup, _Chem. Phys._ , _29_ , 383 - 390 (1978).

5) N. R. Kestner, J. Logan, and J. Jortner, _J. Phys. Chem._ , _78_ , 2148 - 2105 (1974).

6) L. N. Grigorov and D. S. Chernavskii, _Biofizika_ , _17_ , 195 - 202 (1972).

7) J. R. Miller, L. T. Calcaterra, G. L. Closs, _J. Am. Chem. Soc._ , _106_ , 3047 - 3049 (1984).

8) A. D. Joran, B. A. Leland, G. G. Geller, J. J. Hopfield, and P. B. Dervan, _J. Am. Chem. Soc._ , _106_ , 6090-6092 (1984).

9) M. R. Wasielewski and M. P. Niemczyk, _J. Am. Chem. Soc._ , _106_ , 5043 - 5045 (1984).

10) L. T. Calcaterra, G. L. Closs and J. R. Miller, _J. Am. Chem. Soc._ , _105_ , 670-671 (1983).

11) J. R. Winkler, D. G. Nocera, K. M. Yocom, E. Bordignon, and H. B. Gray, _J. Am. Chem. Soc._ , _104_ , 5798-5800 (1982).

12) J. L. Y. Kong and P. A. Loach , _J. Heterocycl. Chem._ , _17_ , 737-744 (1980).

13) J. L. Y. Kong, K. G. Spears and P. A. Loach , _Photochem. Photobiol._ , _35_ , 545-553 (1982).

14) I. Tabushi, N. Koga and M. Yonagita, _Tetrahedron Lett._ , _20_ , 257 -260 (1979).

15) T. F. Ho, A. R. MacIntosh and J. r. Bolton , _Nature_ , _286_ , 254 - 256 (1980).

16) A. Siemiarczuk, A. R. McIntosh, Te-Fu Ho, M. J. Stillman, K. J. Roach, A. C. Weedon, J. R. Bolton and J. S. Connolly, _J. Am. Chem. Soc._ , _105_ , 7224-7230 (1983).

17) A. R. McIntosh, A. Siemiarczuk, J. R. Bolton, M. J. Stillman, Te-Fu Ho, A. C. Weedon, _J. Am. Chem. Soc._, _105_, 7215-7223 (1983).

18) M. Migita, T. Okada, N. Mataga, S. Nishitani, N. Kurata, Y. Sakata, S. Misumi, _Chem. Phys. Lett._, _84_, 263 - 266 (1981).

19) S. Nishitani, N. Kurata, Y. Sakata, S. Misumi, M. Migita, T. Okada, N. Mataga, _Tetrahedron Lett._, _22_, 2099-2102 (1981).

20) C. E. D. Chidsey and S. G. Boxer, _Biophys. J._, _33_, 172 (1981).

21) N. Mataga, A. Karen, T. Okada, S. Nishitani, N. Kurata, Y. Sakata, and S. Misumi, _J. Phys. Chem._, _88_, 5138 - 5141 (1984)

22) M. A. Bergkamp, J. Dalton, and T. L. Netzel, _J. Am. Chem. Soc._, _104_, 253 - 259 (1982).

23) E. B. Fleischer, _Acc. Chem. Res._, _3_, 105 (1970).

24) S. Silvers and A. Tulinsky, _J. Am. Chem. Soc._, _88_, 927 (1964).

25) K. Kalyanasundaram and M. Neumann-Spallart, _J. Phys. Chem._, _86_, 5163 - 5169 (1982)

26) K. Simolo, Ph D. Thesis, University of Rochester (1985).

27) F. R. Hopf and D. G. Whitten in "Porphyrins and Metallo Porphyrins" (ed. K. M. Smith), pp. 667-700. New York: Elsevier Scientific Publishing (1975).

28) H. B. Gray, personal comunication

29) R. A. Marcus, _Disc. Far. Soc._, _29_, 21 - 31 (1960).

30) R. A. Marcus, _J. Chem. Phys._, _43_, 679-701 (1965).

31) R. A. Marcus, _Ann. Rev. Phys. Chem._, _15_, 155-196 (1964).

32) K. Kalyanasundaram and M. Neumann-Spallart, _J. Phys. Chem._, _86_, 5163 - 5169 (1982).

33) The lowest energy of visible transition in the ruthenium complexes onsets at ≈ 3 eV.

34) M. R. Wasielewski, personal comunication

35) B. Chance, D. DeVault, H. Frauenfelder, R. A. Marcus, J. R. Schrieffer, and N.

Sutin, (eds.) "Tunneling in Biological Systems", New York: Academic Press (1979).

36) J. R. Miller, J. Y. Beitz, and R. Kurt Huddleston, <u>J. Am. Chem. Soc.</u>, <u>106</u>, 5057 - 5068 (1984).

37) D. Mauzerall, <u>Israel Journal of Chemistry</u>, <u>21</u>, 321 - 324 (1981).

38) M. D. Newton and N. Sutin, <u>Ann. Rev. Phys. Chem.</u>, <u>35</u>, 437 - 480 (1984).

39) D. LeRoux, J. C. Mialocq, O. Anitoff and G. Folcher, <u>J. Chem. Soc., Faraday Trans.</u>, <u>80</u>, 909-920 (1984).

40) R. A. Marcus and P. Siders, personal communication

41) M. Gouterman, in "The Porphyrins" David Dolphin (editors), Academic Press, Inc., New York, pp. 1-156 (1978).